ETHYLENE ADSORPTION ON MODIFIED BENTONITE

Saran Youngjan

A Thesis Submitted in Partial Fulfillment of the Requirements for the

Degree of Master of Science in Chemistry

Suranaree University of Technology

Academic Year 2012

การดูดซับเอทิลีนบนเบนโตไนต์ที่ถูกดัดแปร

นายศรัณย์ ยวงจันทร์

วิทยานิพนธ์นี้เป็นส่วนหนึ่งของการศึกษาตามหลักสูตรปริญญาวิทยาศาสตรมหาบัณฑิต

สาขาวิชาเคมี

มหาวิทยาลัยเทคโนโลยีสุรนารี

ปีการศึกษา 2555

ETHYLENE ADSORPTION ON MODIFIED BENTONITE

Suranaree University of Technology has approved this thesis submitted in partial fulfillment of the requirements for a Master's Degree.

Thesis Examining Committee

_____

(Assoc. Prof. Dr. Jatuporn Wittayakun)

Chairperson

_____

(Asst. Prof. Dr. Kunwadee Rangsriwatananon)

Member (Thesis Advisor)

_____

(Asst. Prof. Dr. Thanaporn Manyum)

Member

_____

(Asst. Prof. Dr. Sanchai Prayoonpokarach)

Member

_____   _____

(Prof. Dr. Sukit Limpijumnong)   (Assoc. Prof. Dr. Prapun Manyum)

Vice Rector for Academic Affairs   Dean of Institute of Science

ศรัณย์ ยวงจันทร์ : การดูดซับเอทิลีนบนเบนโตไนต์ที่ถูกดัดแปร (ETHYLENE ADSORPTION ON MODIFIED BENTONITE) อาจารย์ที่ปรึกษา : ผู้ช่วยศาสตราจารย์ ดร.กุลวดี รังษีวัฒนานนท์, 81 หน้า.

งานนี้มุ่งเน้นการดูดซับเอทิลีนด้วยเบนโตไนต์ที่ถูกดัดแปร ซึ่งเตรียมจากวิธีที่แตกต่างกัน 3 วิธี เพื่อให้เกิดเป็นวัสดุที่มีรูพรุน ได้แก่ ออร์แกโนเคลย์ พิลลาร์เคลย์ (PILC) และวัสดุเฮทเทอร์โร สตรัคเจอร์ที่เป็นพอรัสเคลย์ (PCHs) โดยออร์แกโนเคลย์เตรียมได้จากการดัดแปรเบนโตไนต์ด้วย สารลดแรงตึงผิวที่แตกต่างกันที่มีความเข้มข้น 3 5 10 และ 20 มิลลิโมลาร์ พิลลาร์เคลย์ที่ใช้ในงาน นี้คือ อะลูมิเนียมพิลลาร์เคลย์และ PCHs 3 ชนิดที่สังเคราะห์ภายใต้เงื่อนไขที่แตกต่างกัน นำมาใช้ใน การดูดซับเอทิลีน ตัวดูดซับทั้งหมดนำมาวิเคราะห์ลักษณะด้วยเทคนิค XRD และ FT-IR และการ วิเคราะห์พื้นผิวด้วยวิธี BET XRD ของเบนโตไนต์ปรากฏพีคที่ 2θ = 5.92° ซึ่งตรงกับระยะห่าง ระหว่างชั้นเท่ากับ 15.08 Å หลังจากการทำพิลลาร์ด้วยอะลูมิเนียม 13 (Al_{13}) ระยะห่างระหว่างชั้น เพิ่มขึ้นเป็น 18.20 Å (2θ = 4.80-5.00°) สำหรับออร์แกโนเคลย์พีคที่ 2θ เลื่อนไปจากในกรณีของ เบนโตไนต์เริ่มต้นเล็กน้อย ส่วนสเปกตราของ PCHs มีลักษณะแตกต่างจากของเบนโตไนต์เริ่มต้น สังเกตได้จากการไม่ปรากฏของพีคที่เป็นลักษณะเฉพาะ ที่ 3632 และ 1039 cm^{-1} สำหรับพื้นที่ผิว จำเพาะ PCHs มีค่าสูงกว่า PILC และออร์แกโนเคลย์ โดยพื้นที่ผิวของเบนโตไนต์มีค่าเท่ากับ 31 m^2/g หลังจากการดัดแปร ออร์แกโนเคลย์ พิลลาร์เคลย์และ PCHs มีพื้นที่ผิวเพิ่มขึ้นเป็น 70 235 และ 897 m^2/g ตามลำดับ

ไอโซเทอร์มการดูดซับเอทิลีนชี้ให้เห็นว่าตัวดูดซับที่ดีที่สุดคือ PCHs ซึ่งสามารถดูดซับเอ-ทิลีนได้ถึง 32 cm^3/g ในขณะที่ออร์แกโนเคลย์และ PILC สามารถดูดซับเอทิลีนได้เพียง 12 และ 13 cm^3/g ตามลำดับ นั่นคือความจุการดูดซับเอทิลีนขึ้นอยู่กับพื้นที่ผิวของตัวดูดซับอย่างมีนัยสำคัญ

สาขาวิชาเคมี   ลายมือชื่อนักศึกษา_____

ปีการศึกษา 2555   ลายมือชื่ออาจารย์ที่ปรึกษา _____

SARAN YOUNGJAN : ETHYLENE ADSORPTION ON MODIFIED

BENTONITE. THESIS ADVISOR : ASST. PROF. KUNWADEE

RANGSRIWATANANON, Ph.D. 81 PP.

BENTONITE /SURFACTANT/ ORGANOCLAY/PILLARED CLAY/ETHYLENE

ADSORPTION

This work focused on the ethylene adsorption on modified bentonite samples prepared in three different ways to produce porous materials namely organoclay, pillared clay (PILC) and porous clay heterostructure materials (PCHs). Organoclay was prepared by modifying bentonite with various surfactants with concentrations of 3, 5, 10 and 20 mM. PILCs used in this work were Al-pillared clays and three samples of PCHs synthesized with different conditions were used in the ethylene adsorption. The adsorbents were characterized by XRD and FT-IR techniques and surface analysis by BET method. XRD pattern of bentonite showed a peak at $2\theta = 5.92°$, corresponding to the basal spacing of 15.08 Å. After pillaring with Al_{13}, the basal spacing was increased to 18.20 Å ($2\theta = 4.80\text{-}5.00°$). For organoclay, the 2θ peak was slightly shifted from the starting bentonite. The spectra of PCHs were different from those of the starting bentonite indicating by the absence of the characteristic peaks at 3632 and 1039 cm^{-1}. The specific surface area of PCHs was higher than that of PILC and organoclay. The surface area of bentonite was 31 m^2/g. After modification the surface area of organoclay, PILC and PCHs was increased to 70, 235 and 897 m^2/g, respectively.

The ethylene adsorption isotherms indicated that the best absorbent was PCHs capable of adsorbing ethylene up to 32 cm^3/g, while organoclay and PILC could adsorb ethylene only 12 and 13 cm^3/g, respectively. This implied that the ethylene adsorption capacity depended significantly on the surface area of adsorbent.
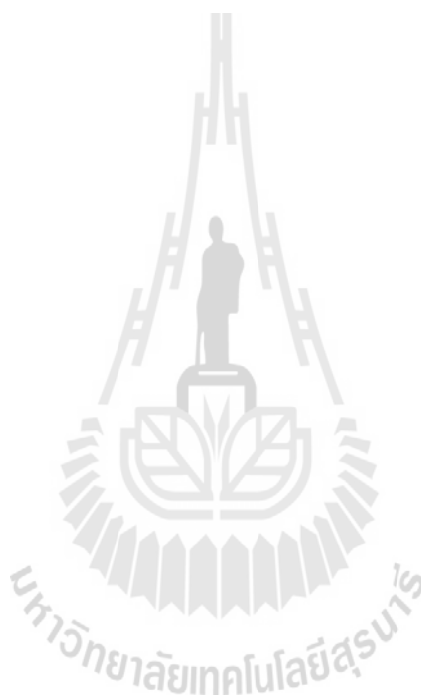
School of Chemistry   Student's Signature_____

Academic Year 2012   Advisor's Signature_____

ACKNOWLEDGEMENTS

CONTENTS

CONTENTS (Continued)

LIST OF TABLES

LIST OF FIGURES

LIST OF FIGURES (Continued)

LIST OF FIGURES (Continued)

LIST OF FIGURES (Continued)

LIST OF ABBREVIATIONS

BET	=	Brunauer–Emmett–Teller
C-1	=	Tetramethylammonium hydroxide
C-2	=	Ethyltrimethylammonium iodide
C-6	=	Hexylmethylammonium bromide
cm^{-1}	=	Per centimeter
cm^3/cc	=	Cubic centimeter
$^{\circ}C$	=	Degree celcius
FT-IR	=	Fourier transforms infrared spectrophotomet
HDTMA	=	Hexadecyltrimethylammonium chloride
K	=	Kelvin
kV	=	Kilovolt
M	=	Molar
mA	=	Milliampere
min	=	Minute
mL	=	Milliliter
mM	=	Millimolar
MTPB	=	Methyltriphenylphosphonium bromide
PCH	=	Porous clay heterostructures
PILC	=	Pillared interlayer clay
PTAB	=	Phenyltrimethylammonium bromide

LIST OF ABBREVIATIONS (Continued)

% T   =   Percent transmittance

TEOS   =   Tetraethyl orthosilicate

Vinyl   =   (Vinylbenzyl)trimethylammonium chloride

XRD   =   X-ray diffraction

CHAPTER I

INTRODUCTION

Ethylene or ethene (IUPAC name) is an alkene with the formula C_2H_4. There is a double bond between two carbon atoms and four single hydrogen-carbon bonds in its structure and the structure is shown in Figure 1.1.
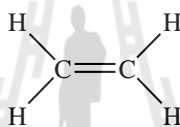
Figure 1.1 Ethylene molecules.

Ethylene is an odorless, colorless and naturally occurring gas. It is extremely important in several reactions, for example, polymerization, oxidation, alkylation, hydration, halogenation, hydrohalogenation, oligomerization, oxo-reaction, etc. and also has a role in biology as a phytohormone that acts at trace level (Chow and McCourt, 2006). Ethylene is produced essentially from all parts of plants, including leaves, stems, roots, flowers, fruits, tubers and seedling. During the life of plants, ethylene production is induced during certain stages of growth such as seed germination, root and shoot growth, ripening of fruits, abscission of leaves and senescence of flowers (Wang et al., 2004). In food and floral industry, the shelf life of harvests can cause significant economic losses for markets, suppliers, and growers. An acceptable visual and organoleptic quality of the harvests is the main point which has to be considered. A number of specific defects which

diminished the valuable in harvest products vary in many ways such as premature ripening and decay, russet spotting, loss of color, odor, wilting, scald and loss of crunch, rind breakdown, bitterness and early sprouting. The defects given above are the examples for unacceptable visual and bad qualities caused by the phytohormone named ethylene.

Accumulation of ethylene may result in a number of specific defects in harvest products. Therefore, removal of ethylene is needed to extend shelf life of harvests to keep their acceptable visual and their organoleptic quality. Ethylene removal is of economic importance to the food and floral industry. It allows producers, handlers and sellers to spread availability over periods of strong and weak demand, maintaining supply and stabilizing cost.

One of the most effective materials to remove ethylene is potassium permanganate and also other materials as the adsorbents for ethylene such as activated carbon (Choi, Choi, and Lee 2003), zeolite X and zeolite Y (Berlier, Olivier and Jadot, 1995) modified zeolite (Patdhanagul, 2010) and clinoptilolite (Erdogan, 2008). However, because of the chemical properties of potassium permanganate, precautions must be taken in order to prevent contamination of food products (Abe and Watada, 1991). To search for materials with ethylene removal capability is our aim to study. Especially, we focused on clays, because they are cheap, eco-friendly and available in large quantity in Thailand. In addition, they can be simply modified to organoclays with surfactants in order to increase their hydrophobicity and can be changed from sheet structure (only bentonite) to two dimensional porous structure. The main question is whether clays or modified clays can be used as adsorbent for removal of ethylene or not. Therefore, the study of ethylene adsorption on clays and modified clays is necessary.

1.1   Clay minerals

Clay minerals consist of small crystalline particles with silica-oxygen tetrahedral sheets and aluminium or magnesium octahedral sheet. Because of isomorphous substitution of silicon ion by aluminium ion in the tetrahedral layers or similar substitution of aluminium ion by magnesium ion, clay minerals have a net negative charge. Thus, cations like sodium, potassium and calcium may be attracted to the mineral surface to neutralize the layer charge. The structure and composition of clay minerals will be described as to be phyllosilicates or sheet silicates with stacking of octahedral and tetrahedral sheets which are the two basic building blocks making up the basic structural units. Each sheet is composed of planes of atoms, a plane of hydroxyls or oxygens and a plane of aluminiums or magnesiums or silicons, arranged one above the other. Variations among clay minerals and differences in their physical and chemical properties arise from the various combinations of octahedral and tetrahedral sheets and the electrostatic effects that chemical substitutions have on the unit.

The common groups of phylloclay minerals occurring in soils and sediments are listed in Table 1.1. The clay mineral structures, based on combination of octahedral and tetrahedral sheets, are of 1:1, 2:1 and 2:1:1 type. In the 1:1 type consisting of one octahedral and one tetrahedral sheet, the plane of apical oxygens of the tetrahedral sheet is superimposed on the OH plane of the octahedral sheet (Figure 1.2). The common plane of junction consists of both oxygen and unshared OH. The unshared OH occurs at the center of each six-fold ring defined by the apical tetrahedral oxygen. The 2:1 type is the stacking of an octahedral sheet sandwiched between two tetrahedral sheets, so that their planes of apical oxygens face toward

each other. The common planes between the two tetrahedral sheets and the octahedral sheets consist of sharing oxygen and unshared OHs, each unshared OH being at the center of tetrahedral apical oxygen hexagonal ring (Figure 1.3). The 2:1:1 structure consists of a 2:1 layer arrangement with an additional octahedral sheet between the 2:1 layers (Clauer and Chaudhuri, 1995).

The thickness of each structural unit depends not only on the number of sheets involved, but also on the compositions of octahedral and tetrahedral sheets and the charge compensations as a result of unbalanced substitutions of cations in the sheet. The net compensating charge may be located either in the interlayer site as in 2:1 layer arrangements or in the additional octahedral sheet in 2:1:1 layer arrangements. The most common interlayer cations are Ca^{2+}, Mg^{2+}, H^+, Na^+, K^+, and NH_4^+. Interlayer sites might also be occupied by Fe and Al in a hydroxyl form.
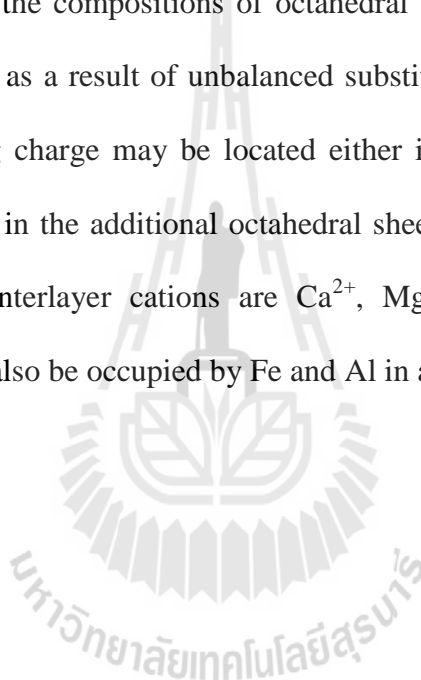
Table 1.1 Classification scheme and ideal chemical composition of clay minerals in soils.

Type	Charge per formula unit	Group	Subgroup and minerals	Ideal chemical composition	
TO (or 1:1)	0	Kaolin-serpentine	Nonexpanding. Dioctahedral series		
			Kaolin subgroup		
			Kaolinite	$Al_4Si_4O_{10}(OH)_8$	
			Dickite	$Al_4Si_4O_{10}(OH)_8$	
			Nacrite	$Al_4Si_4O_{10}(OH)_8$	
			Nonexpanding. Trioctahedral series		
			Serpentine subgroup		
			Chrysotile	$Mg_6Si_4O_{10}(OH)_8$	
			Antigorite	$Mg_6Si_4O_{10}(OH)_8$	
			Lizardite	$Mg_6Si_4O_{10}(OH)_8$	
			Amesite	$(Mg_4Al_2)(Si_2Al_2)O_{10}(OH)_8$	
			Expanding. Dioctahedral series		
			Kaolin subgroup		
			Halloysite	$Al_4Si_4O_{10}(OH)_8 \cdot 4H_2O$	
TOT (or 2:1)	0	Talc-pyrophyllite	Nonexpanding. Dioctahedral series		
			Pyrophyllite	$Al_4Si_8O_{20}(OH)_4$	
			Nonexpanding. Trioctahedral series		
			Talc	$Mg_6Si_8O_{20}(OH)_4$	
TOT (or 2:1)	0.25-0.6	Smectite	Expanding. Dioctahedral series		
			Beidellite	$[(Al_{4.0})Si_{7.5-6.8}$	$Al_{0.5-1.2})$ $O_{20}(OH)_4]Na_{0.5-1.2}$
			Montmorillonite	$[(Al_{3.5-2.8}$	$Mg_{0.5-1.2})$ $(Si_8)O_{20}(OH)_4]Na_{0.5-1.2}$
			Nontronite	$[(Fe_{4.0})(Si_{7.5-6.8}$	$Al_{0.5-1.2})$ $O_{20}(OH)_4]Na_{0.5-1.2}$
			Expanding. Trioctahedral series		
			Hectorite	$[(Mg_{5.5-4.8}$	$Li_{0.5-1.2})$ $(Si_{8.0})O_{20}(OH)_4]Na_{0.5-1.2}$
			Saponite	$[(Mg_{6.0})(Si_{7.5-6.8}$	$Al_{0.5-1.2})$ $O_{20}(OH)_4]Na_{0.5-1.2}$
TOT (or 2:1)	0.6-0.9	Vermiculite	Expanding. Dioctahedral series		
			Vermiculite	$[(Al_{4.0})(Si_{6.8-6.2}$	$Al_{1.2-1.8})$ $O_{20}(OH)_4]Na_{1.2-1.8}$
			Expanding. Trioctahedral series		
			Vermiculite	$[(Mg_{6.0})(Si_{6.8-6.2}$	$Al_{1.2-1.8})$ $O_{20}(OH)_4]Na_{1.2-1.8}$
		Illite	Nonexpanding. Dioctahedral series		
			Illite	$[(Al_{4.0})(Si_{7.5-6.5}$	$Al_{0.5-1.5})$ $O_{20}(OH)_4]K_{0.5-1.5}$
[TOT]O[TOT] (or 2:1:1)	Variable	Chlorite	Nonexpanding. Dioctahedral series There is some evidence for the existence of such a mineral, e.g., donbassite Nonexpanding. Trioctahedral series Chlorites with structures relates to $[(Mg,Fe)_{3-x}(Al,Fe)_x(Si_{4-x}Al_x)O_{10}(OH)_2]$ e.g., Cliochlore		

Source: Shmuel and Harold, 2002.
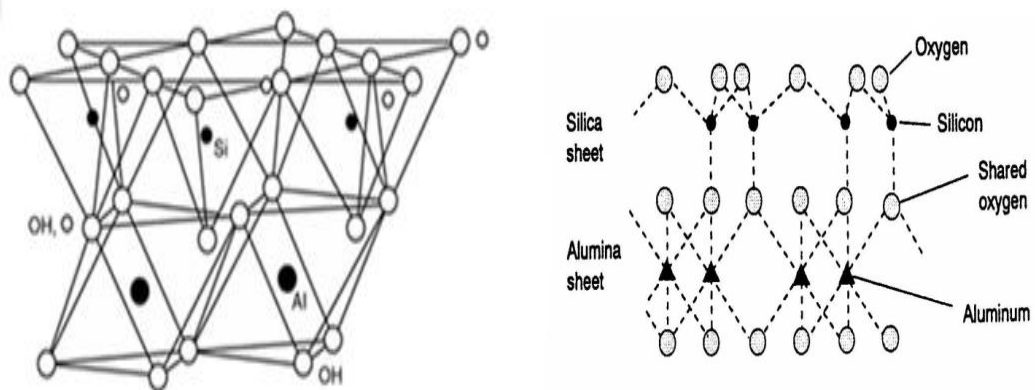
Figure 1.2 Schematic representation of the crystal structure of a 1:1 type clay mineral.

Source: Shmuel and Harold, 2002.
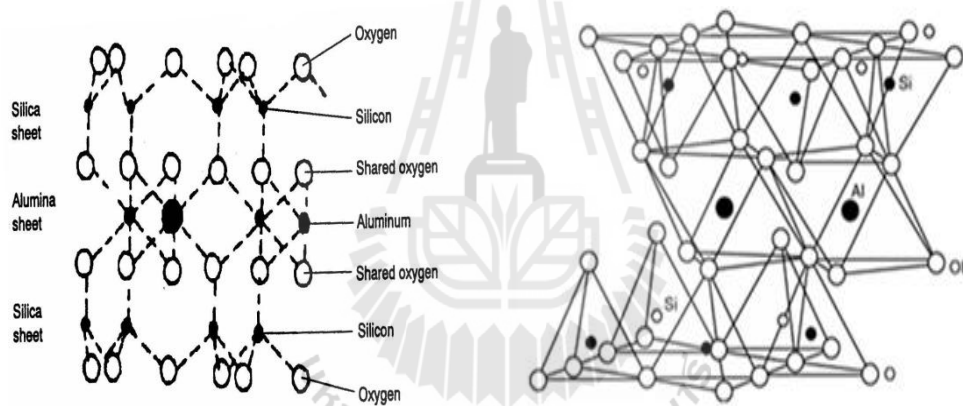
Figure 1.3 Schematic representation of the crystal structure of a 2:1 type clay mineral.

Source: Shmuel and Harold, 2002.

Montmorillonite is an aluminosilicate with a layer structure, classified as phyllosilicate. The layer structure is composed of one aluminium octahedral layer sandwiched between two silicon tetrahedral layers. The tetrahedral sheet is composed of silicon-oxygen tetrahedral linked to neighboring tetrahedral by sharing three corners to form a hexagonal network (Figure 1.4). The fourth corner of each

tetrahedron (the apical oxygen) points into and forms a part of the adjacent octahedral sheet. The octahedral sheet is usually composed of aluminium or magnesium in six-fold coordination with oxygen from the tetrahedral sheet and with the hydroxyl group. Individual octahedral is linked laterally by sharing edges (Figure 1.5). Tetrahedral and octahedral sheets taken together form a layer, which may join to each other in a clay crystallite by interlayer cations, using Van der Waals and electrostatic forces, or hydrogen bondings (Grim, 1953; Izumi, Urabe and Onaka, 1992; Spark, 1995).
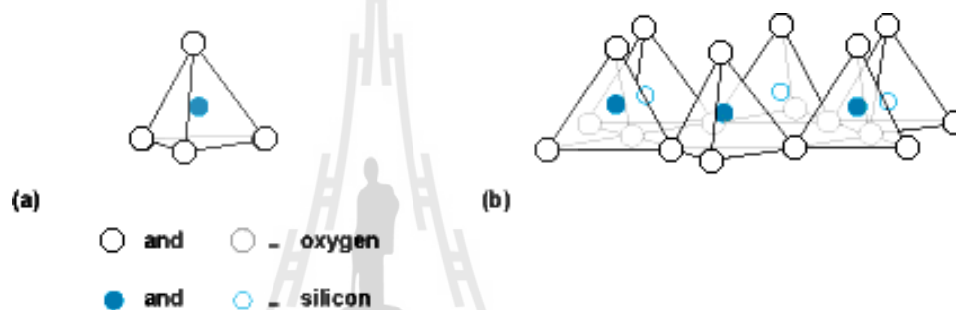
Figure 1.4 Diagrammatic sketch showing (a) single silica tetrahedron and (b) sheet structure of silica tetrahedrons arranged in a hexagonal network.

Source: Grim, 1953.
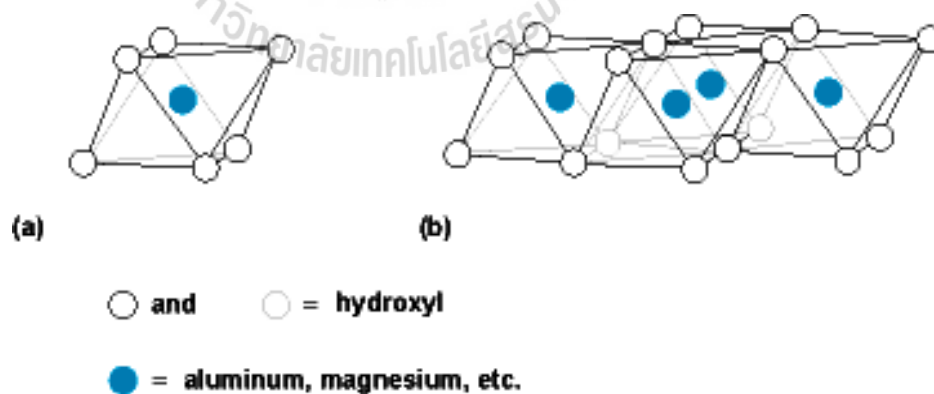
Figure 1.5 Diagrammatic sketch showing (a) single octahedral unit and (b) sheet structure of octahedral units.

Source: Grim, 1953.

Bentonite usually forms from weathering of volcanic ash with the chemical formula $Al_2O_3 \cdot 4SiO_2 \cdot H_2O$. Bentonite is clay consisting predominantly of smectite minerals, usually montmorillonite. Generally, cation exchange capacity (CEC) of bentonite varies between 80 and 150 meq/100 g and about ten times higher than that of the other clay minerals. About four-fifths of the CEC relates to the exchangeable interlayer cation and the rest to bonds at the edges of the crystallites. Bentonites are also known for their ability to dehydrate and rehydrate repeatedly in continental weathering and soil environments because of fluctuating moisture condition (Clauer and Chaudhuri, 1995).
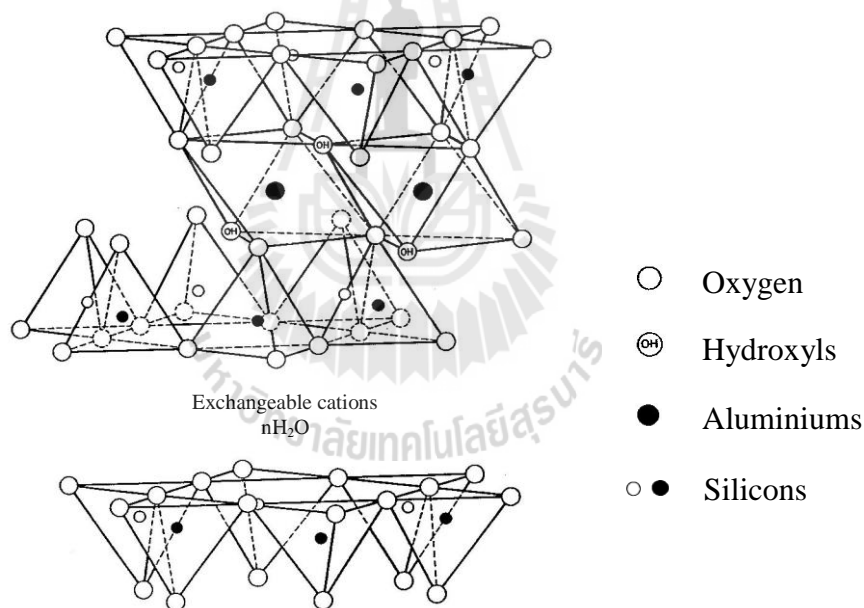
Figure 1.6 Structure of the bentonite.

Source: Grim, 1953.

1.2   Organoclays

The interactions between organic compounds and clay minerals are among the most widespread reaction in nature. The adsorption of organic materials by clay

minerals has been widely investigated during the last decade. The interactions include cation exchange and adsorption of polar and nonpolar molecules. Adsorption is a primary process, in which physical or chemical bonds (long- or short- range interactions, respectively) are formed between the mineral and the organic matter. In most adsorption reactions the clay minerals serve as the substrates and the organic entities are the adsorbed species. This is true for clay particles with sizes larger than those of the organic entities. However, in the case of huge polymers with very high molecular weights, such as cellulose, the clay particles may be located in the organic web. In this case the polymer web should be considered as the substrate and the clay particle as the adsorbed material (Shmuel and Harold, 2002).

Organoclays are synthesized by grafting cationic surfactants onto clay minerals. Cationic surfactants are usually quaternary ammonium compounds such as $[(CH_3)_3NR]^+$ or $[(CH_3)_2NRR']^+$ where R and R' are alkyl or aryl groups. The interlaminar distance of the d_{001} plane of the clay, which has not been organically modified, is relatively small, and the interlayer environment is hydrophilic. Intercalation of organic surfactant between layers of the clay not only changes them from hydrophilic to hydrophobic, but also greatly increases the basal spacing of the layers. The increased basal spacing together with hydrophobic surface makes organoclay an effective material for ethylene adsorption (Kukkadapu and Boyd, 1995; Lawrence, Kukkadapu and Boyd, 1998).

In nature, the negative structural charge is balanced by exchangeable cations such as Na^+, Ca^{2+}, etc at the aluminosilicate surfaces. Cation exchange reaction starts at the edges of clay particle and then spreads toward the center in a highly regular fashion. The charge on the clay layers and its location (octahedral or

tetrahedral) will influence the strength of the electrostatic attraction between layers and mobility of interlayer space. At the same time, reaction rates are influenced by the size and valence of the exchanging inorganic cations. When highly charged silicates are saturated with larger, less hydrated, monovalent cations such as K^+, Rb^+, NH_4^+, and Cs^+, the attraction between layers is greatest. When the layers are saturated with Na^+, Li^+, Ca^{2+} and Mg^{2+} which have larger hydration energies, then the attraction between the layers will be overcome and the basal spacing will be increased. Even complete dissociation can occur. Small highly hydrated cations are more mobile and easier to replace since inorganic cations have relatively high hydration energies and usually several layers of water molecules will be associated with them (Johnston, Sposito and Erickson, 1992).

In addition, the concentration of sorbed organic cations usually can reach as much as cation exchange capacity (CEC) of clays. Some authors have however reported that the organic cations are generally sorbed on charged 2:1 layer silicates in excess of the cation exchange capacity of the clay. When organic cations replace hydrated inorganic cations, the silicate surface is changed from hydrophilic to hydrophobic. The organic cations can adhere to isomorphic substitution site via electrostatic interactions or they can adhere to the sorbed organic cations by van der Waals forces (Marguls, Rozen and Nir, 1988).

The arrangement of organic cations in organoclay depends on the size of organic cations, for instance the length of alkyl chain and charge of the clay minerals (Lagaly, 1982). Generally, in adsorptive clays, the organic cations only form monolayers. In the case of organophilic clays, the organic cations may form monolayers, bilayers, pseudotrimolecular layers or paraffin complexes. These

arrangements of organic cations also affect the basal spacing of organic clays which can be analyzed by XRD. For example, in the case of HDTMA, the C-16 alkyl chain may form monolayers to paraffin complexes, corresponding to the basal spacing d_{001} of 13.7 Å, 17.7 Å, 21.7 Å and >22 Å, respectively.

The different interlamellar arrangements of alkylammonium ions are as follows (Bonczek, Harris and Nkedi, 2002; Maksimov, Gaidukovs and Kalnins, 2006).

Monolayers: When the packing density of the chains is low, the chains are assumed an arrangement with the C-C-C plane parallel to the layers, the chains will lie parallel to the silicate layers. The characteristics basal spacing is 13.6 Å. This spacing is often observed for short alkylammonium ions.

Bilayer: The chains are parallel to the silicate layer. Typical basal spacing is 17.6 Å.

Pseudotrimolecular layers: The polar end groups of the alkylammonium ions remain attached to the layers. By formation of kinks the unpolar chain ends are shifted one above the other and the interlayer separation is determined by the thickness of tree alkyl chains. The basal spacing is about 22 Å.

Paraffin-type layers: The ammonium groups remain attached to the silicate layer, the chains in all *trans*-conformation point away from the surface.
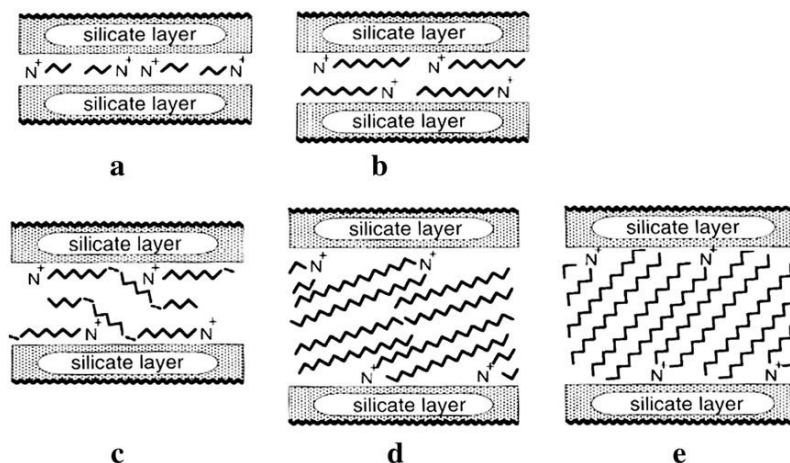
Figure 1.7 Orientation of alkylammonium ions in the galleries of layered silicate: (a) monolayer, (b) bilayers, (c) pseudotrimolecular layers, and (d, e) paraffin-type arrangements of alkylammonium ions with different tilting angles of the alkyl chains

Source: Bergaya, Theng and Lagaly, 2006.

1.3   Pillared clays

Pillared clays (PILC) are materials with permanent porosity, obtained by propping the elementary clay sheets with a chemical substance, called molecular prop. A cross-linked clay or CLC, in particular a cross-linked smectite or CLS, is a PILC with chemical bonds between the prop and the surface oxygen of the clay. A CLC or CLS is thus a special case of PILC.

The goal of the pillaring process is to introduce microporosity in the system. The dimensions of the micropores are complementary to those of zeolites (>0.70 nm and <2.0 nm). It is easy to achieve pillared clay by replacement of the interlayer exchangeable cations in smectite clay by metal complex cations which are converted by calcination into oxide pillars between the clay layers. Other application of

modified montmorillonite is to make pillared clay which is two-dimensional layer material developed in the late 1970s as a catalyst for crude oil cracking processes. Various kinds of metal-PILC have been introduced such as Al-PILC, Zr-PILC, Cr-PILC, Si-PILC, Fe-PILC and Ti-PILC (Wibulswas, White and Rautiu, 1999).

The concept of pillaring is very straightforward and consists of two main steps. Firstly, the interlamellar small cations are exchanged for other, bulky ions. A second step or calcination step converts the inorganic polyoxycation precursors into rigid, stable metal oxide pillars, tightly bonded to the clay layers (Figure 1.8).

It has became clear that both the parent clay and the pillars must possess several properties in order to allow the pillaring process to be successful. The clay should have a moderate cation exchange capacity to obtain the best swelling and alkali or alkaline earth ions in the interlayer space can easily be exchanged. From this point of view, smectites are the ideal host. The pillaring cation requires a high positive charge and must be dissolvable in the polar solvent used to swell the clay.
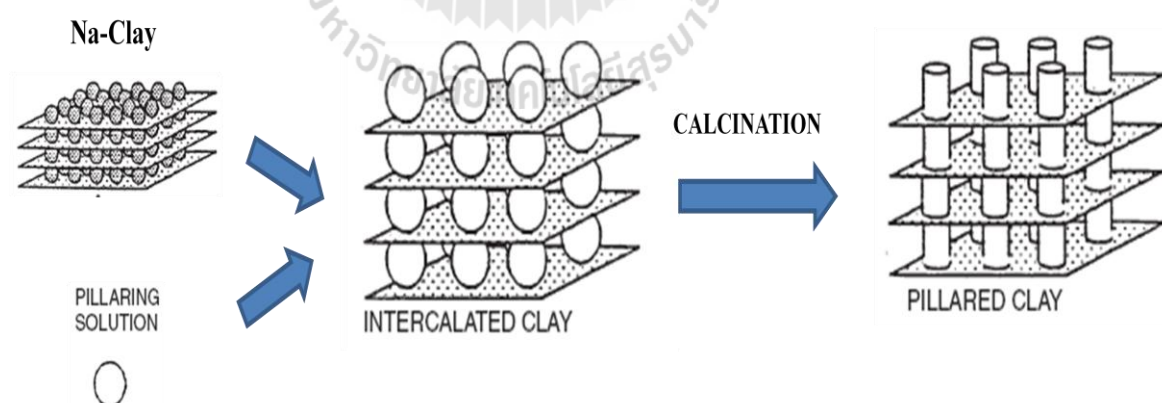
Figure 1.8 The principle of pillaring.

Source: Cool and Vansant, 1998.

Nowadays, the pillaring of clays is a well established technique in the preparation of new porous solids. It is an easy and controllable way to introduce porosity in a rather inexpensive substrate. A variety of pillaring species is available, all with specific sizes and compositions. In this way, it is possible to prepare PILCs with different interlayer free spacings which determine the pore size. The interpillar distance can be tuned by varying the charge of both host and pillars.

Depending on the final purpose of the material, the appropriate pillar can be chosen. This flexibility in the PILC synthesis is one of the main advantages compared to other porous substrates, such as zeolites, which have one definite pore size. The technique not only focuses on clays, but other layered structures serve as host materials as well. Examples are layered double hydroxides (anionic clays), metal (IV)-phosphates and phosphonates, layered silicic acids, etc.

The most popular and most useful pillaring cations are the polyoxycations. They are synthesized by a controlled hydrolysis of metal salts to give complexes with the desired properties for pillaring: high charge, bulky character, and convertible to stable oxide pillars upon heating. Table 1.2 gives an overview of the most common PILCs together with their characteristics. Figure 1.9 shows some typical pillaring precursors.

Among them, only the Al-PILC exhibits a narrow pore size distribution (Maes and Vansant, 1995). The hydrolysis is the easiest to control, and the pillar dimensions are not very sensitive to the differences in the hydrolysis conditions. Interlayer free spacings between 7 and 10 Å are always obtained.

Table 1.2 Properties of pillared clays intercalated with polyoxycation pillars.

Pillar species	Surface area (m^2/g)	Interlayer free spacing (Å)
Al_2O_3	200–400	7–10
ZrO_2	200–300	4–14
Cr_2O_3	300	12
Fe_2O_3	100–300	15 (Mesopores)
TiO_2	300	14–18 (Mesopores)

Source: Cool and Vansant, 1998.
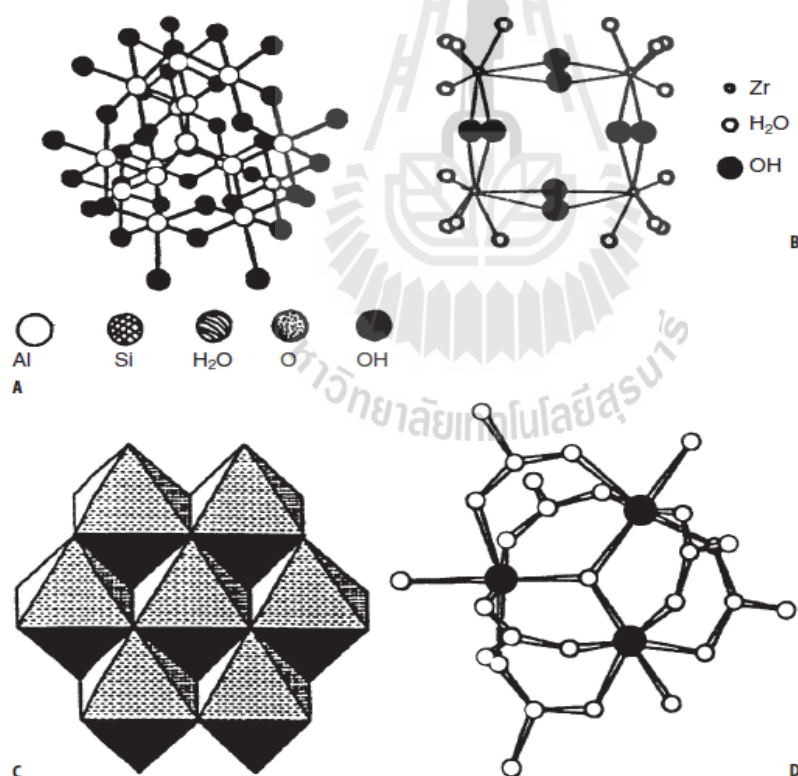
Figure 1.9 Illustration of some pillaring precursors for Al-PILC (A), Zr-PILC (B), Ti-PILC (C) and Fe-PILC (D).

Source: Cool and Vansant, 1998.

1.4   Characterization techniques

1.4.1   X-ray Diffraction (XRD)

X-ray diffraction is one of the most important and most powerful methods in the primary investigation for identifying the variety of crystalline mineral species present in the clay fraction of soils (Bergaya, Theng and Lagaly, 2006). This method is based on the scattering of x-rays by the electrons of atoms. The wavelengths of x-rays are similar to interatomic distances and so the x-rays scattered by different atoms will interfere destructively, in the latter case giving rise to diffracted beams. In mineralogical studies, the diffracted x-rays are used to measure the dimensions of the atomic layers in the crystals. Since each different mineral has a distinct set of atomic layer spacings (called d-spacings), the suite of measurements can be used to identify the mineral. All crystalline minerals in the sample can be identified from one XRD scan, if they are present in sufficient abundance (Lewis and McConchie, 1994). The geometry of the corresponding diffraction events can be described by Bragg's law:

$$n\lambda = 2d\sin\theta \tag{1}$$

where the integer n is the order of the diffracted beam which can be any whole number, λ is the wavelength of the incident x-ray beam, d is the distance between adjacent planes of atoms (the d-spacings), and θ is the angle of incidence of the x-ray beam. Known values of λ and θ can be used to calculate the d-spacings. The geometry of an XRD unit is designed to accommodate this measurement (Figure 1.10). The characteristic set of d-spacings generated in a typical x-ray scan provides a unique "fingerprint" of the mineral or minerals present in the sample. When properly

interpreted, by comparison with standard reference patterns and measurements, this "fingerprint" allows for the identification of the material.
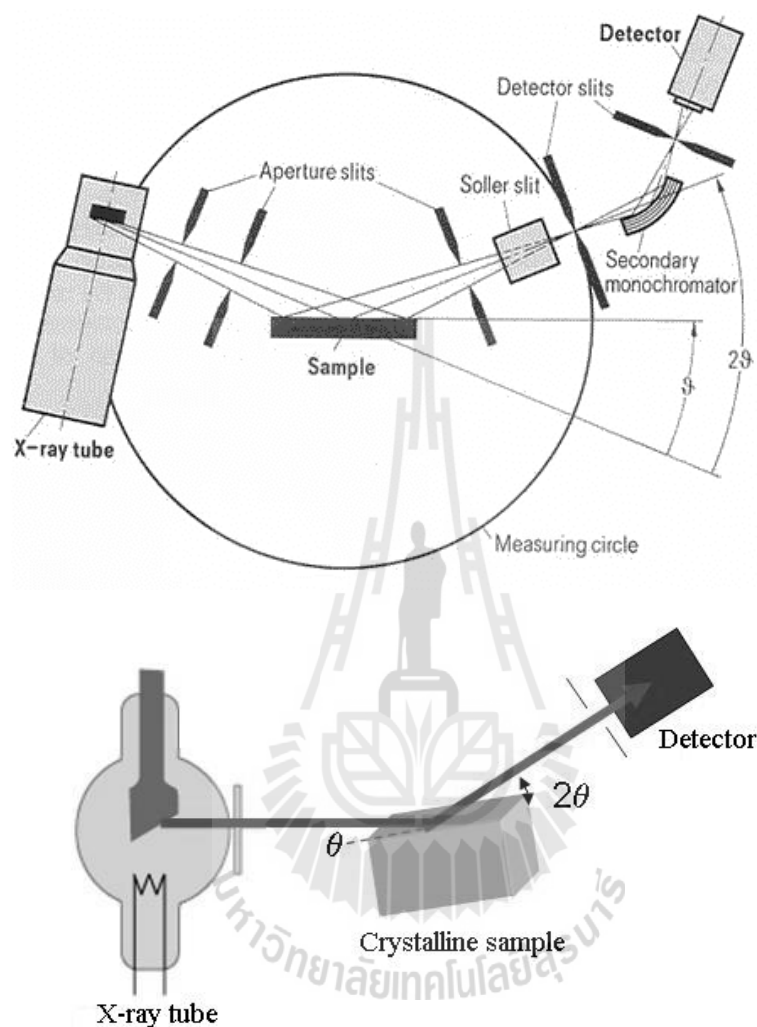
Figure 1.10 The schematic diagram of x-ray diffraction.

Source: Department of Chemistry, Northern Kentucky University, www, 2012.

1.4.2 Fourier transform infrared spectroscopy (FTIR)

FTIR can be used to confirm surface characteristics and isomorphous substitution by other elements of clay materials and to derive information concerning their structures, compositions and structural changes upon chemical modification (Madejov′a, 2003; Russell and Fraser, 1994; Velde, 1992). Infrared radiation is used

to probe the energy levels of molecules. The total energy of a molecule can be thought of as a combination of transitional, vibrational, rotational, and electronic energies. These types of molecular energies are quantized, and only discrete energy levels are permitted. Therefore, molecules absorb energy inputs only at those nonarbitrary levels. Infrared energy corresponds to rotational and vibrational transitions of molecules. Since molecules in solid rarely rotate freely, IR studies of minerals are primarily concerned with vibrational transitions (Olson, Thompson and Wilson, 2000). For FTIR analysis, the background spectrum of a KBr pressed pellet is firstly recorded, then followed by measuring the sample, pressed and diluted (2%) in KBr. The mid-infrared region of the spectrum (4000-400 cm^{-1}) is the most interesting part of the spectrum when dealing with siliceous materials as it contains the fundamental framework vibrations of the $Si(Al)O_4$ groupings. Identification of materials in this region is possible because different materials will absorb at different frequencies. In addition to the characteristic nature of the absorptions, the magnitude of the absorption in the spectrum due to a given species can be related to the concentration of that species (quantitative analysis).

1.4.3 Determination of surface area

The BET theory is a well-known theory for the physical adsorption of gas molecules on a solid surface (Do, 1998). The concept of the theory is an extension of the Langmuir theory, which is a theory for monolayer molecular adsorption to multilayer adsorption with the following hypotheses; gas molecules physically adsorb on a solid in layers infinitely, there is no interaction between each adsorption layer and; the Langmuir theory can be applied to each layer. The resulting BET equation is expressed by

$$\frac{1}{V\left[\dfrac{P}{P_0}-1\right]} = \frac{1}{V_m c}\left(\frac{P}{P_0}\right) + \frac{1}{V_m} \qquad (2)$$

P and P_0 are the equilibrium and the saturation pressures of adsorbates at the temperature of adsorption, V is the adsorbed gas quantity (for example, in volume units), and V_m is the monolayer adsorbed gas quantity. c is the BET constant, which is expressed by

$$c = \exp\left(\frac{E_1 - E_L}{RT}\right) \qquad (3)$$

E_1 is the heat of adsorption for the first layer, and E_L is that for the second and higher layers and is equal to the heat of liquefaction. Equation (2) is an adsorption isotherm and can be plotted as a straight line with $1/V\left[\dfrac{P}{P_0}-1\right]$ on the y-axis and $\dfrac{P}{P_0}$ on the x-axis according to experimental results. The linear relationship of equation is kept in the range of $0.05 < \dfrac{P}{P_0} < 0.35$. This plot is called a BET plot. The values of the slope and the y-intercept of the line are used to calculate the monolayer adsorbed gas quantity V_m and the BET constant c. The BET method is widely used in surface science for the calculation of surface area of solids by physical adsorption of gas molecules. A total surface area, S_{total}, and a specific surface area, S, are evaluated by the following equations:

$$S_{total} = \frac{(V_m Ns)}{M} \tag{4}$$

$$S = \frac{S_{total}}{w} \tag{5}$$

where N is Avogadro's number, s is adsorbate cross section, M is molecular weight of adsorbate, and w is weight of solid sample.

1.4.4 Determination of pore volume

The total pore volume is derived from the amount of vapor adsorbed at a relative pressure close to unity. By assuming that the pores are filled with liquid adsorbate, if the adsorbate contains no macropores the isotherm will remain nearly horizontal over the range of P/P_0 approaching unity and the pore volume is well defined. However, in the presence of macropores, the isotherm rises rapidly near P/P_0 equal to 1 and in the limit of large macropores the isotherm may exhibit an essentially vertical rise. The limiting adsorption can be identified reliably assuming that it is the total pore volume. The nitrogen adsorption isotherm can be used to determine the pore volume. The volume of nitrogen adsorbed (V_{ads}) can be converted to the volume of liquid nitrogen (V_{liq}) contained in the pores using equation below:

$$V_{liq} = \frac{P_a V_{ads} \overline{V}}{RT} \tag{6}$$

in which P_a and T are ambient pressure and temperature, respectively, $\overline{V}$ is the molar

volume of the liquid adsorbate for nitrogen and $\overline{V}$ is equal to 34.7 cm^{3}mol^{-1}.

1.4.5   Determination of pore size

Since pores which would not be filled below a relative pressure equal to

1 have a negligible contribution to the total pore volume and the surface area of the

adsorbent, the average pore size can be estimated from the pore volume. The average

pore radius, r_p,can be expressed as

$$r_p = \frac{2V_{liq}}{S} \tag{7}$$

where V_{liq} is obtained form equation (6) and S is the BET surface area.

1.4.6   Determination of micropore surface area

A t-plot is a plot of the volume of gas adsorbed versus the statistical

thickness of an adsorbate film. The thickness is calculated as a function of the relative

pressure according to the de Boer equation.

$$t = a\left[\frac{1}{\ln\left(\frac{P_0}{P}\right)}\right]^{\frac{1}{b}} \tag{8}$$

Here, t is the statistical thickness, and the terms a and b are 6.0533 and 3.0 for

nitrogen adsorption at 196 °C, respectively. If adsorbates have no micropores, it is

evidenced by the ability to extrapolate the line to the origin. In contrast, if micropores

are present, the t-plot will exhibit a positive intercept as shown in Figure 1.11.

micropore absence   micropore presenc
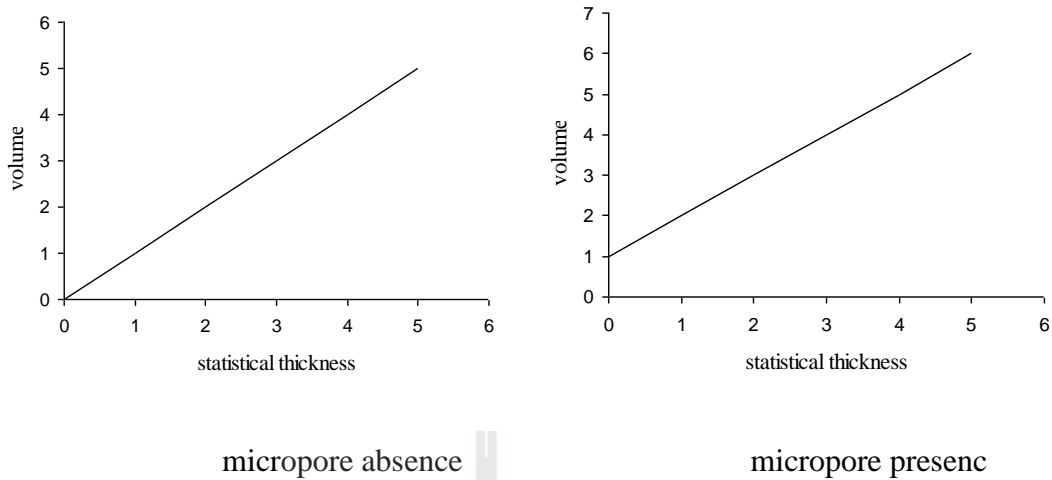
Figure 1.11 The t-plot.

Source: Do, 1998.

Since the slope represents the total surface area of all pores, that is

$$S_{total} = \frac{V_{ads}^{STP}(15.47)}{t} \tag{9}$$

where V_{ads}^{STP} is the volume of gas adsorbed corrected to standard conditions of temperature and pressure. The constant 15.47 represents the conversion of the gas volume to liquid volume. Using the slope s of the plot in the case of adsobate having no micropores, the equation (9) is reduced to

$$S_{total}\left(m^2 g^{-1}\right) = s \times 15.47 \tag{10}$$

The intercept I, when converted to a liquid volume, gives the micropore volume V_{mp}. That is

$$V_{mp} = I \times 0.001547 \left(cm^3 \right) \tag{11}$$

The micropore surface area, S_{mp}, is the difference between the BET surface area and the external surface area S_{ext} from the t-plot. That is

$$S_{mp} = S_{BET} - S_{ext} \tag{12}$$

The instrument used to analyze surface area, pore volume and pore size data is Autosorb-1C, Quantachrome. The schematic of the instrument is shown in Figure 1.12.

Figure 1.12 Flow diagram of adsorption instrument.

Source: Quantachrome Instruments, www, 2010.

Firstly, the sample was outgased at sample preparation station for a suitable period. Then, the sample was moved to analysis station. In analysis step, at the adjusted P/P_0, firstly nitrogen gas was flushed to the analysis cell that contains

sample. The sample adsorbed some nitrogen gas and released the excess nitrogen gas out. The following step is measuring the released nitrogen gas and calculating the difference between the amounts of nitrogen flushed and released. This difference is the amount of nitrogen adsorbed onto the sample surface at the adjusted P/P_0. In commonl, for BET measurement, 7 points of P/P_0 (0.05 to 0.35) are usually required and at P/P_0 equal to 1 the pore volume and pore size are measured. The nitrogen adsorption isotherm and the BET plot are illustrated in Figure 1.13.
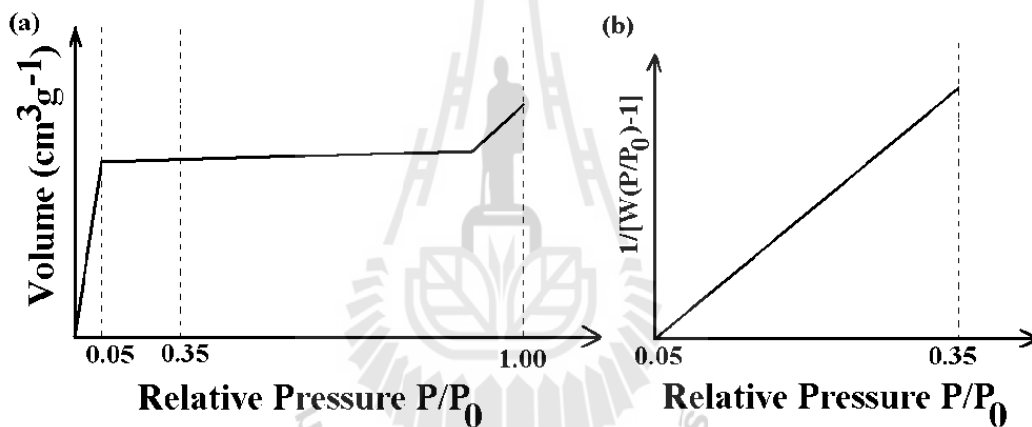
Figure 1.13 Plot of (a) nitrogen adsorption isotherm and (b) BET.

Source: Do, 1998.

1.5   Research objectives

1.3.1   To prepare organobentonite samples by different quaternary ammonium ions with different concentrations.

1.3.2   To prepare aluminium pillared clay and porous clay heterostructure material.

1.3.3   To characterize all of the prepared samples with different techniques: XRD, FT-IR and Brunauer-Emmett-Teller (BET).

1.3.4   To study the ethylene adsorption on the prepared sample
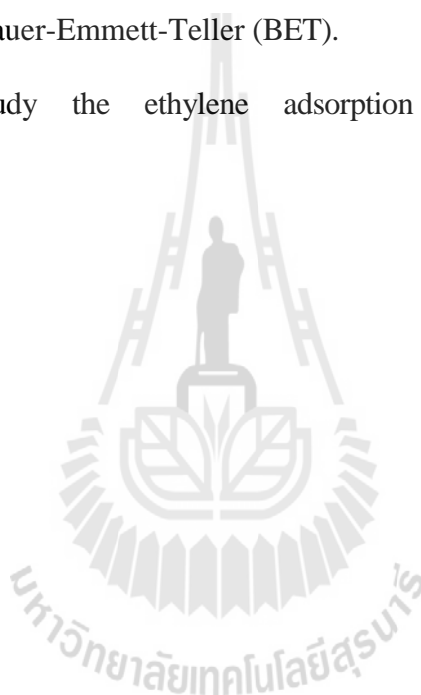
CHAPTER II

LITERATURE REVIEWS

There are many researches that studied the modification of clay minerals with surfactants to organoclays to increase their hydrophobicity on the surface for adsorbing effectively organic compounds and some researchers studied the modification of clays to porous materials to enhance their surface areas for an increase in an adsorption capability of gas molecules.

Modifications of bentonite with HDTMA were widely used for removing organic compounds (Richards and Bouazza, 2007; Upson and Burns, 2006). This study revealed that organobentonite could act as a successful adsorbent for removing the aromatic organics from contaminated soil. Majdan, Bujacka and Sabah, (2009) showed the clear difference in adsorption of phenol on phenyltrimethylammonium (PTMA)- and benzyltrimethylammonium (BTMA)-bentonite. The inspection of the FT-IR spectrum of BTMA-bentonite loaded with phenol in the regions of 1300-1600 and 1620-1680 cm^{-1} showed the features of π–π electron interaction between the benzene ring of phenol and the BTMA cation together with the phenol-water hydrogen bond.

Wang et al. (2004) studied the surfactant ion exchange effect on the pore structure, surface characteristics and adsorption properties of montmorillonite. Ca-montmorillonite was exchanged with two quaternary amines, tetramethylammonium chloride (TMA) and hexadecyltrimethylammonium bromide (HDTMA). They found

that the exchange processes might induce an increase or decrease in the surface area, pore size and pore volume of montmorillonite, depending on the size, the molecular arrangement and the degree of hydration of the exchanged ion in the clay. Gitipour, Bowers and Bodocsi, (1997) investigated the clay-aromatic interactions by using bentonite to bind benzene, toluene, ethylbenzene and *o*-xylene in contaminated soils.

Alkaram, Mukhlis and Al-Dujaili, (2009) reported the removal of phenol from aqueous solution by using modified bentonite and kaolinite with hexadecyltrimethylammonium bromide (HDTMA) and phenyltrimethylammonium bromide (PTMA) surfactants. It was found that the removal of phenol from aqueous solutions by modified clays seemed to be more effective than unmodified samples.

Zielke and Pinnavaia (1988) modified the pillared, delaminated and hydroxyl interlayered smectites. Further, it was used for the removal of chlorinated phenols from aqueous solutions. Srinivasan and Fogler (1990) applied the organoclays in the removal of benzo(α)pyrene and chlorophenols from industrial wastewaters. The montmorillonite was pillared with the help of inorganic aluminium ion (Al_2O_3) and hence, the surface of the montmorillonite as well the pillared montmorillonite was modified using hexadecyl pyridine. These solids were employed for the removal of phenol from aqueous solutions. The results indicated that both organo modified solids enhanced greatly the uptake of phenols. Moreover, the adsorption capacity of pillared montmorillonite was greatly dependent on the presence of micropores and specific surface area available in the modified clay (Wu, Liao, Zhang and Guo, 2001). They further, proposed the recycling of the PMt materials by calcining at 350 °C and again modified with the surfactant molecule. In a line alumina pillared clays and mesomorphous alumina, aluminium phosphate was applied in the removal of

chlorinated phenols from aqueous solutions (Danis, Albanis, Petrakis and Pomonis, 1998).

The pillaring of the clay materials with the inorganic metals viz., Al, Fe, Cr, Ti etc. showed good settling property, but very little affinity towards the organics in the aqueous solutions. However, the complete modification of these intercalated clays with organic cationic surfactants possessed fairly a good sorption capacity for the organic pollutants (Bouras et al., 2002; El-Nahhal et al., 1998; Wibulswas et al., 1999). Important features of these inorgano/organo-clays were reported that they possessed two different sorption sites capable of removing different types of pollutants i.e., organic and inorganic pollutants from the aqueous solutions simultaneously apparently, with an enhanced sorption capacity (Ma and Zhu, 2006; Yan, Shan, Wen and Owens, 2008).

A porous clay heterostructure (PCH) was prepared and characterized, and its aqueous phenol and dichlorophenols (DCPs) adsorption capacities was studied. The PCH displayed a surface area of 305.5 m^2/g, average porous diameter of 37.2 Å and a basal space of 23.2 Å. The adsorption capacity shown by the PCH for both phenol and (DCPs) from water suggested that the PCH had both hydrophobic and hydrophilic characteristics (Arellano-Cardenas, Gallardo-Velazquez1 and Osorio-Revilla, 2007).

Porous materials were obtained from clays by gallery templated synthesis. The surface areas of the samples were in the range of 600-700 m^2/g and the corresponding microporous volumes were near 0.3 cm^3/g. The possibility of using such materials as adsorbents of volatile organic compounds, due to their textural and hydrophobic characteristics, was studied by comparing the adsorption of ethanol, methyl ethyl ketone and water (Pires et al., 2004).

Mixtures of light olefins and paraffins produced in the petroleum refining process are often used as refinery fuel (Eldridge, 1993). Yang and Kikkinides (1995) reported the most promising results among the previous attempts on the sorbents for olefin/paraffin separation by adsorption via π-complexation. They showed that on the Ag^+ resin at 25 °C and 1 atm, C_2H_4 adsorption capacity was 1.15 mmol/g, and the equilibrium adsorption ratio for C_2H_4/C_2H_6 was 9.2. Cheng and Yang (1995) dispersed cuprous chloride on pillared interlayered clays (PILC). Among them, $CuCl/TiO_2$-PILC adsorbent was the best which showed a C_2H_4/C_2H_6 adsorption ratio of 5.3 and C_3H_6/C_3H_8 2.9 at 1 atm and 25 °C. Although the olefin/paraffin adsorption ratios on the PILC sorbent were not as high as those on the Ag-resin, they yielded a steeper portion above the knee of the isotherm and more rapid adsorption rates.

Al-Baghli and Loughlin (2006) reported experimental data and a model predictions for the binary adsorption of ethylene and ethane on Engelhard titanosilicate (ETS-10). Their results suggested that the adsorptive separation of ethylene from ethane was very favorable on ETS-10.

Anson, Wang, Lin, Kuznicki and Kuznicki, (2008) studied the adsorption of ethane and ethylene on modified Engelhard titanosilicate. Engelhard titanosilicate was modified by ion exchange with different mono-, di-, and trivalent cations. It was found that ethylene/ethane adsorption selectivity decreased in the order Na>K>Li>Cu≈Ba>Ba/H>La/H.

Pires, Araujo, Carvalho, Pinto, Gonzalez-Calbet and Ramırez-Castellanos, (2008) studied the adsorption of CO_2, CH_4, C_2H_6 and N_2 on pillared clays (PILC) which were prepared from two different natural montmorillonite clays, by pillaring with Al_2O_3 and ZrO_2. They found that the surface area of the clays pillared with Al_2O_3

was higher than that of the clays pillared with ZrO_2. At the highest studied equilibrium pressure, the order of maximum adsorption was found to be $CO_2>C_2H_6>CH_4>N_2$ for each material.

The adsorbent for ethylene with natural clinoptilolite (Erdogan, Sakızci and Yorukogullari, 2008), and modified zeolite Y with surfactants (Patdhanagul, Srithanratana, Rangsriwatananon and Hengrasmee, 2010) were reported. It was found that the natural clinoptilolites had a considerable potential for the removal of ethylene (Erdogan et al., 2008) including high ethylene adsorption of NaY (Patdhanagul et al., 2010). When zeolite NaY modified with phenyltrimethylammonium bromide was used as adsorbent, amount of ethylene adsorbed was higher than that on the unmodified one.

Saini, Pinto and Pires, (2011) reported that bentonite was tailored in three different ways to produce porous materials viz. PCH1, PCH2, and PILC. Surface characterization of these materials showed that PCHs had higher surface area than PILC, and had micro and mesoporosity. The adsorption isotherms of ethylene on these materials were measured up to high pressure under different temperatures and, by processing the obtained data, these materials were evaluated for their aptness for ethane ethylene- separation.

CHAPTER III

MATERIALS, INSTRUMENTATION AND

EXPERIMENTAL METHODS

This chapter is divided into three parts. The first part refers to the lists of chemicals and apparatus. The second part mentions the analytical instruments used to characterize the samples. The third part describes the experimental methods.

3.1 Material lists

3.1.1 Chemicals

(a) Bentonite, Thai Nippon Chemical Industry Co., Ltd.

(b) Phenyltrimethylammonium bromide, $C_9H_{14}NBr$, Acros Organics

(c) (Vinylbenzyl)trimethylammonium chloride, $C_{12}H_{18}NCl$, Aldrich

(d) Methyltriphenylphosphonium bromide, $C_{19}H_{18}PBr$, Aldrich

(e) Tetraethylammonium hydroxide, $C_8H_{21}NO$, Fluka

(f) Ethyltrimethylammonium iodide, $C_5H_{14}NI$, Fluka

(g) Sodium hydroxide, NaOH, Merk

(h) Aluminium chloride, $AlCl_3$, QRëC

(i) Cetyltrimethylammonium bromide, $C_{19}H_{42}NBr$, Acros organics

(j) Decylamine, $C_{12}H_{27}N$, Aldrich

(k) Tetraethylorthosilicate, $Si(OC_2H_5)_4$, Aldrich

(l) Hexadecyltrimethylammonium chloride, $C_{19}H_{42}NCl$, Fluka

3.1.2   Apparatuses

(a) Vacuum filtration apparatus (Gast)

(b) Furnace (CWF 1200, Carbolite)

(c) Oven for drying sample (Binder, ED)

(d) Analytical balance (Mettler Toledo)

(e) Desiccators

(f) Standard sieve 230 mesh (63 μm) (Analysensieb, Retsch, USA)

(g) Glass microfiber filters, whatman GF/C diameter 47 mm

(h) Nylon Membrane filters, vertical diameter 13 mm

3.2   Instrumentation

3.2.1   X-ray powder diffraction (XRD)

The adsorbent structure was determined by x-ray diffraction technique using XRD Bruker D5005 Powder XRD with Ni-filtered Cu Kα radiation source and operated at 35 kV/35 mA. The intensity data were collected in a 2θ range from 5° to 30° with the scan rate and step size of $0.5°s^{-1}$ and $0.02°step^{-1}$.

3.2.2   Fourier transform infrared spectroscopy (FT-IR)

.   Infrared spectra were obtained by using a Perkin-Elmer spectrum GX-FTIR Spectrophotometer and infrared spectra were taken in the range of mid infrared (4000-400 cm^{-1}). The solid sample and KBr were dried at 110 °C for 12 h before obtaining the spectra. The sample and KBr were mixed using a mortar and pestle. The ground powder was pressed into a transparent disk using a hydraulic pressing machine

with an equivalent weight of about 10 tons for 2 min. The spectra were obtained by using an average of 10 scans with 4 cm^{-1} resolution.

3.2.3 Surface area, pore volume and pore size

Surface area of the adsorbents was determined by Brunauer-Emmet-Teller (BET) method at temperature of liquid nitrogen -196 °C. The measurement was carried out with Autosorb-1-C instrument (Quantachrome). Prior to each measurement, the 200 mg of adsorbent was degassed at 300 °C for 3 h. The total pore volume and average pore size were determined at relative pressure P/P_0 equal to 1. The external surface area was determined by t-plot method at relative pressure P/P_0 ranging from 0.2 to 0.5. The instrument used to analyze surface area, pore volume and pore size was Autosorb-1C, Quantachrome. The surface analysis data are shown in Chapter IV.

3.3 Experimental methods

3.3.1 Preparation of starting materials

The clay minerals used in this study were kaolin, halloysite and bentonite obtained from the Thai Nippon Chemical Industry Co. They were prepared by sieving to yield particles smaller than 63 μm and dried at 110 °C before using in the further steps (3.3.2-3.3.4).

3.3.2 Preparation of organoclay

Organoclays (organobentonite, organokaolin and organohalloysite) were prepared by using surfactants in an ion exchange process. Organobentonite was prepared by modification of bentonite with hexadecyltrimethylammonium chloride (HDTMA), phenyltrimethylammonium bromide (PTAB),

(vinylbenzyl)trimethylammonium chloride (vinyl), methyltriphenylphosphonium bromide (MTPB), tetraethylammonium hydroxide (C-1), ethyltrimethylammonium iodide (C-2) and hexylmethylammonium bromide (C-6) in the concentration ranging from 0.3 mM to 20.0 mM. Bentonite and cationic surfactants were mixed together and stirred for 48 h. The mixture was centrifuged at 3500 rpm for 20 min and filtered. Then the solid was washed with deionized water (DI) and dried at 110 °C for 3 h. Organokaolin and organohalloysite were prepared by modification of kaolin and halloysite only with HDTMA and phenyltrimethylammonium bromide (PTAB) with concentration of 6 and 12 mM. The data of ethylene adsorption on organokaolin and organohalloysite were shown in Appendix.

3.3.3 Synthesis of Al-pillared bentonite

The preparation of the aluminium-pillared bentonite was modified from the literature (Yan et al., 2008). Firstly, the Al_{13} oligomer with the molar ratio of $OH^-/Al^{3+} = 2.4$ under different conditions was prepared by adding 0.2 M NaOH drop by dropwise to 0.2 M $AlCl_3$ solution under vigorous stirring at ambient temperature and at 70 °C for 1 day and 3 days. The pillared clays were then synthesized by adding the mixtures mentioned above to 2% of clay suspension until the ratio of aluminium to clay was 5 and 10 mmol/g and stirred for 24 h. The intercalations of the pillar were improved by repeated washing with DI water until free of chloride. The pillared clay was then dried, ground and heated at 350 °C for 3 h. The synthesized Al-pillared clays under various conditions are shown in Table 3.1.

Table 3.1 The parameters for preparation of PILCs.

Sameple	Time (day)	mmol Al_{13}	Temp. °C	Ratio: OH^-/Al^{3+}
PILC-1	1	5	ambient temperature	2.4
PILC-2	1	10	ambient temperature	2.4
PILC-3	3	5	ambient temperature	2.4
PILC-4	3	10	ambient temperature	2.4
PILC-5	1	5	70	2.4
PILC-6	1	10	70	2.4

3.3.4 Synthesis of porous clay heterostructures (PCHs)

The method of preparing PCHs was adopted from literature (Pires et al., 2004; Pinto and Rocha, 2008). A suspension of 1 g bentonite in 100 mL distilled water was mixed with 4.8 mL solution of 0.5 M cetyltrimethylammonium bromide (CTAB) solution. The solution was stirred for 12 h at 50 °C and then centrifuged-washed repeatedly until pH~7 to separate the solid from the solution. Then, the solid was added with decylamine (Aldrich, 95%) and stirred for 20 min, after that 35.5 mL of tetraethylorthosilicate, TEOS, (Aldrich, 98%) was added and stirred for 12 h. The obtained suspension was then centrifuged and air dried, after that the sample was calcined at 650 °C for 5 h with a slow ramp (1 °C/min). The different samples of PCH were prepared by varying the proportion volume of 0.5 M CTAB, decylamine and TEOS, as shown in Table 3.2.

Table 3.2 The different volumes of CTAB and decylamine for preparation of PCHs.

Sample	0.5 M CTAB (mL)	Decylamine (mL)	TEOS (mL)
PCH A	4.8	5.3	35.5
PCH B	4.8	10	35.5
PCH C	2.4	5.3	35.5

3.3.5 Ethylene adsorption capability

The capability of ethylene gas adsorption was studied using Nova 1200e instrument (Quantachrome) at 0 °C. The 200 mg adsorbent was degassed at 300 °C for 3 h prior to the measurement. The ethylene adsorption isotherms were determined at relative pressure P/P_0 between 0 and 1. 28 adsorption points and 22 desorption points were measured to create adsorption isotherm. The parameters which were set for ethylene adsorption measurement are described in Table 3.3.

Table 3.3 Ethylene adsorption parameters.

Parameter	Set value
Adsorbate temperature	0 °C
Molecular weight and cross section area	28.05 g mol^{-1} and 0.2310 nm^2 mol^{-1}
Liquid density and molecular density	1.147 g cm^{-3} and 2.00 × 10^{-29} cm^3 mol^{-1}
Critical temperature and pressure	10 °C and 49.7 atm
Average diameter	0.353 nm
Polarizability	1.46 × 10^{-24} cm^3 mol^{-1}
Magnetic susceptibility	6.70 × 10^{14} mol cm^{-3}
Surface tension and contact angle	8.85 erg cm^{-1} and 0.00 degree
Non ideality factor	1.00 × 10^{-5} mmHg^{-1}

In this study, the ethylene adsorption isotherm is classified as type I isotherm. The ethylene adsorption isotherms were measured by Nova 1000e. The ethylene adsorption isotherm of bentonite and their modified which are shown in chapter IV.
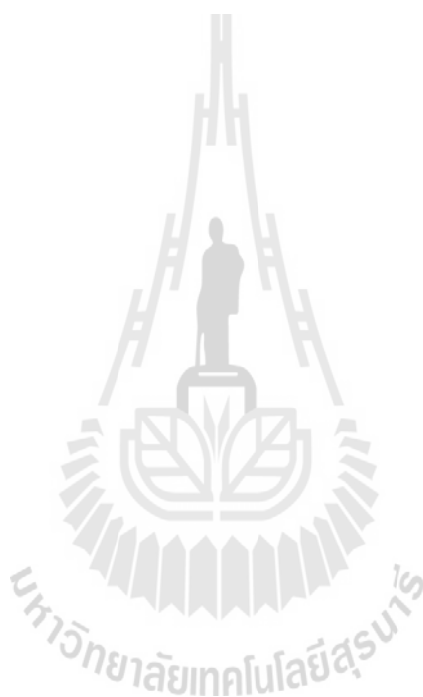
CHAPTER IV

RESULTS AND DISCUSSION

This chapter described and discussed the experimental results. It is divided into 3 parts namely, characterization of modified bentonite, specific surface area analysis and the ethylene adsorption study.

4.1 Standard characterization

4.1.1 FT-IR of bentonite

The most distinctive feature of the bentonite spectrum is the broad absorption band that ranges from 3400-3600 cm^{-1} (Figure 4.1). The band at 3632 cm^{-1} is attributed to the characteristic O-H vibration of bentonite. The band at 3436 cm^{-1} is due to H-O-H stretching of water molecules forming hydrogen bond in the interlayer region of bentonite and the bending vibration mode of water is 1637 cm^{-1}. A band at 1039 cm^{-1} is assigned to the stretching vibration of Si-O groups and the bands at 520 and 470 cm^{-1} correspond to bending vibrations of Al-O-Si and Si-O-Si, respectively. The band at 622 cm^{-1} is assigned to coupled Al-O and Si-O out-of-plan vibration (Eren and Afsin, 2008).
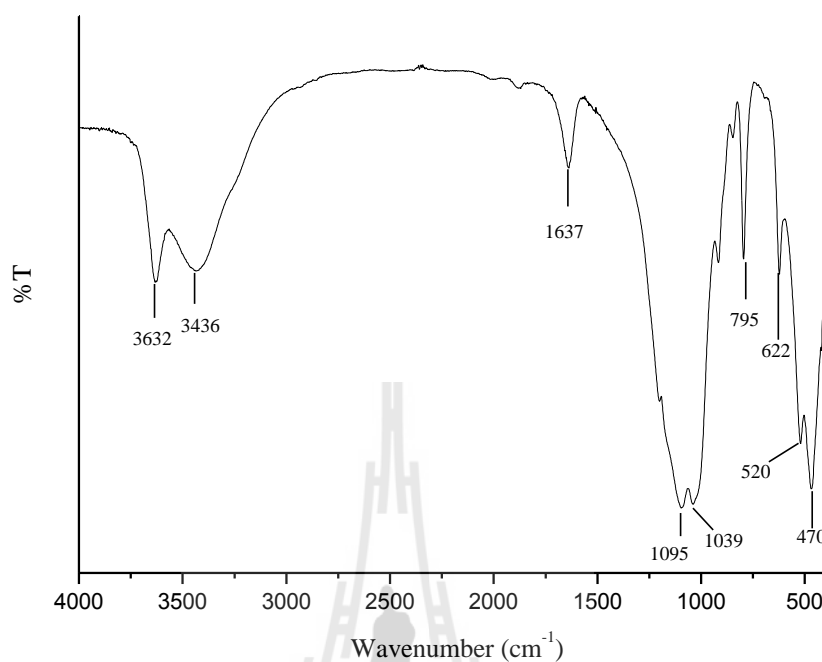
Figure 4.1 FT-IR patterns of bentonite.

4.1.2 Characterization of organobentonite by XRD

The X-ray diffraction patterns of bentonite and the modified bentonites are displayed in Figure 4.2-4.7. The natural bentonite showed a reflection peak at about $2\theta = 5.92°$ which corresponds to a basal spacing of $d_{001} = 15.08$ Å. In the case of organobentonites modified by C-1, C-2, PTAB and Vinyl the 2θ slightly shifted to the angle of $6.41°$ - $6.65°$, $6.12°$- $6.27°$, $5.84°$- $6.03°$ and $5.97°$- $6.03°$ with the concentrations of 3 and 20 mM, respectively, and basal spacing of d_{001} decreased to 13.26-13.77 Å, 14.03-14.42 Å, 14.64-15.12 Å and 14.63-14.81 Å, respectively. The decrease in the basal spacing of d_{001} may be caused by an attractive intermolecular forces between the neighboring sheet, due to the modifiers (C-1, C-2, PTAB, and

Vinyl), sufficiently to keep the sheets close together. The modifiers of C-1 and C-2 brought stronger attractive intermolecular force compared to the others leading to the significant reduction of interlayer spacing of d_{001}. Whereas the modification of TMPB dramatically shifted 2θ to $5.27°$, $5.22°$ and $5.16°$ with higher concentration of 5, 10 and 20 mM, respectively. The d_{001} shifted from 15.08 Å to 17.12 Å. The increase in the interlayer spacing is due to the intercalation of a big molecule of TMPB which composes of three branches of aromatic rings, into the interlayer of the structure.
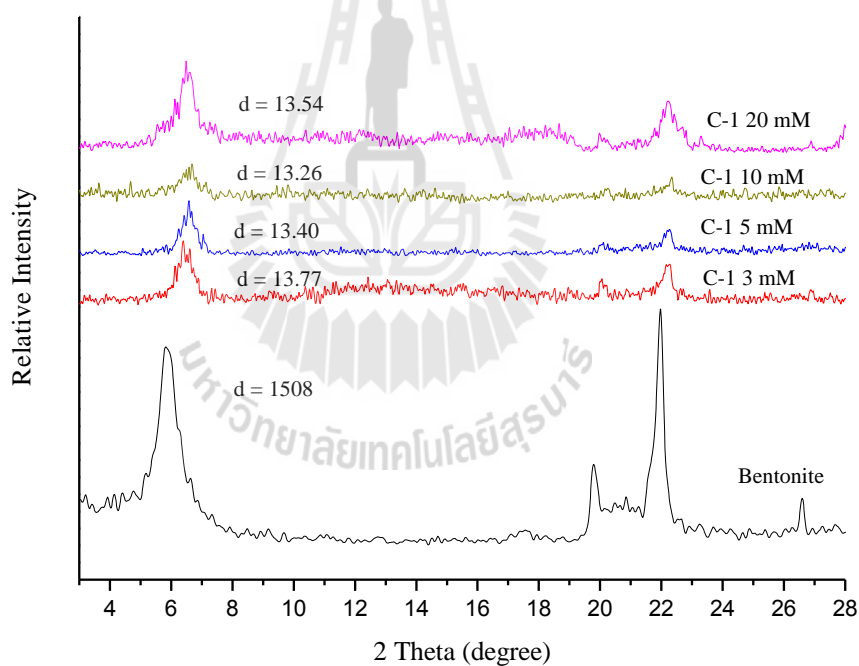
Figure 4.2 XRD patterns of bentonite samples modified by different concentrations of tetramethylammonium hydroxide (C-1).
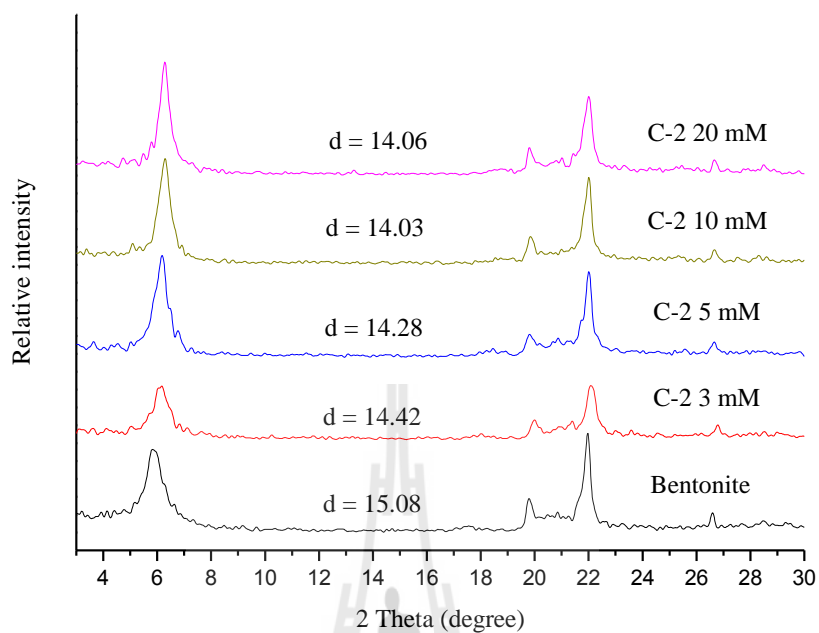
Figure 4.3 XRD patterns of bentonite samples modified by different concentrations of ethyltrimethylammonium iodide (C-2).
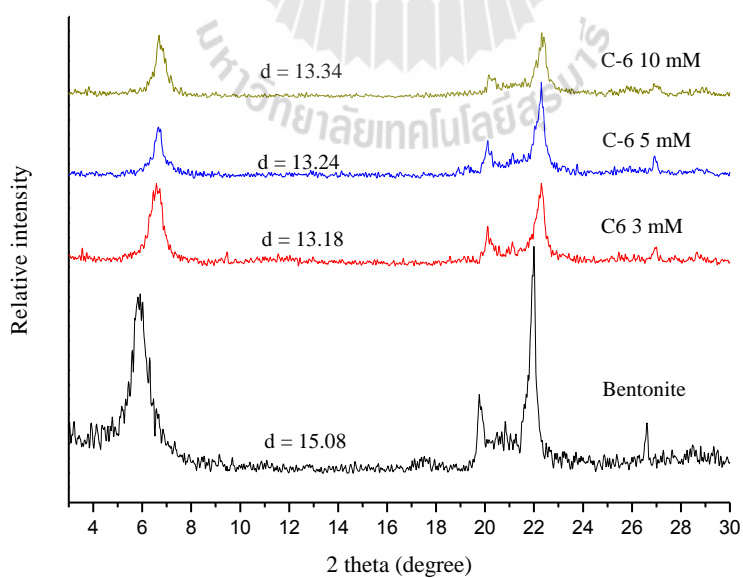
Figure 4.4 XRD patterns of bentonite samples modified by different concentrations of hexylmethylammonium bromide (C-6).
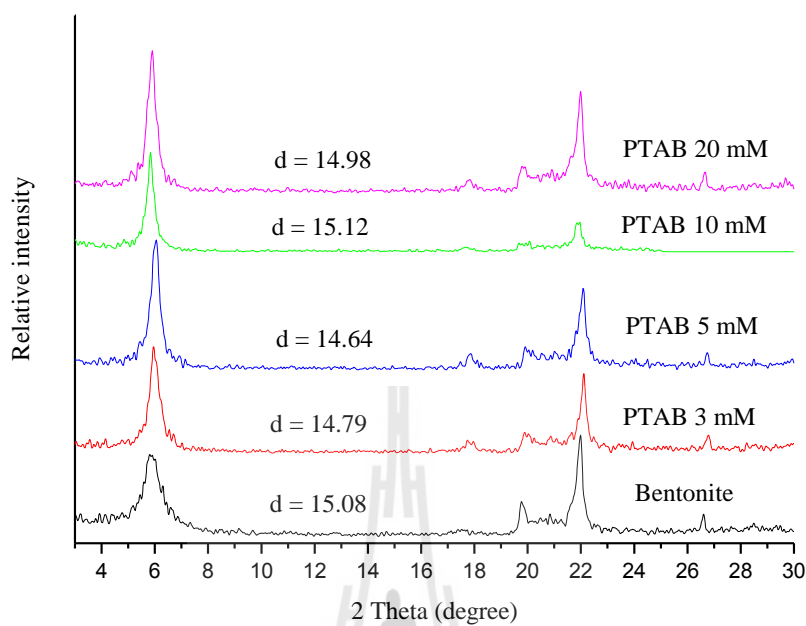
Figure 4.5 XRD patterns of bentonite modified by different concentrations of phenyltrimethylammonium bromide (PTAB).
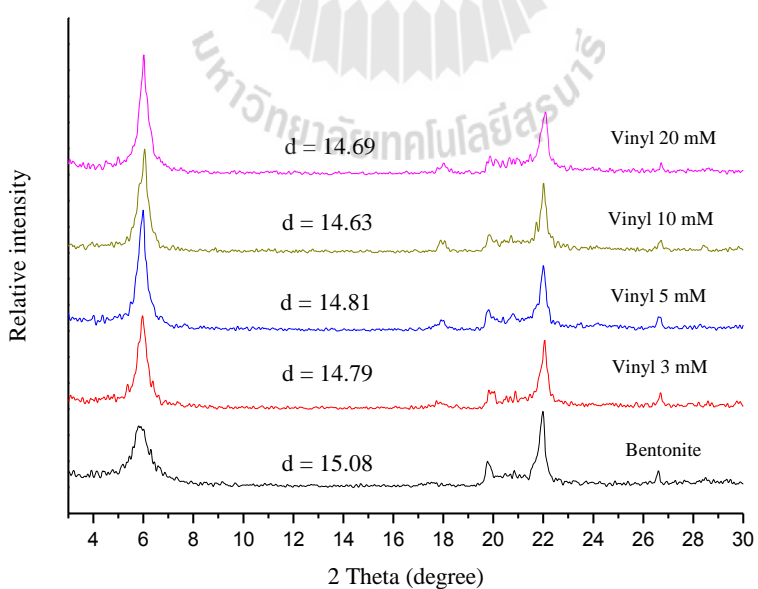
Figure 4.6 XRD patterns of bentonite modified by different concentrations of (vinylbenzyl)trimethylammonium chloride (Vinyl).
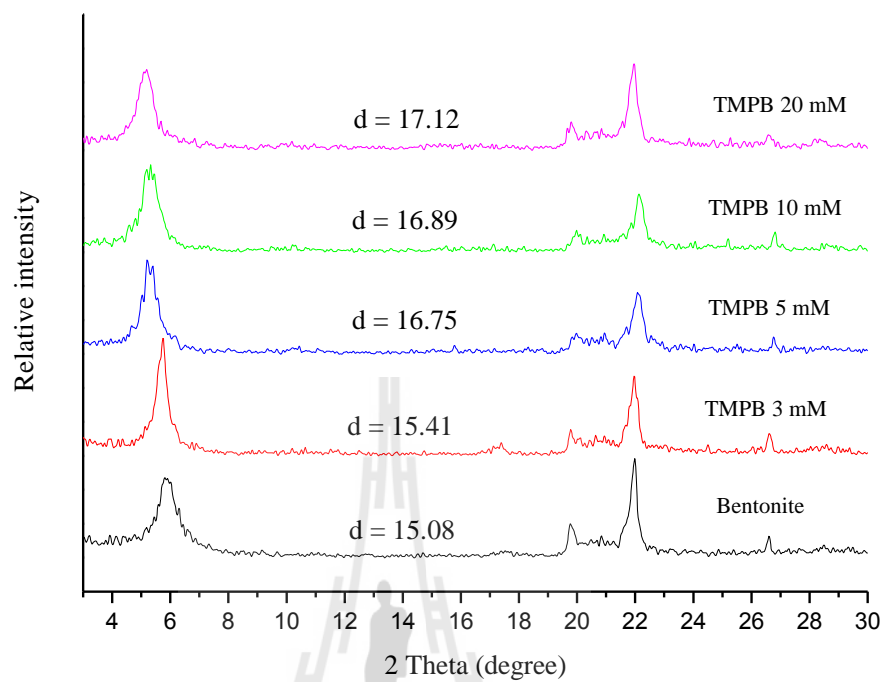
Figure 4.7 XRD patterns of bentonite modified by different concentrations of methyltriphenylphosphonium bromide (MTPB).

Table 4.1 The basal spacing d_{001} of organoclay.

Sample	Concentration (mM)	d-spacing (Å)
Bentonite	-	15.08
C1-bentonite	3	13.77
	5	13.40
	10	13.26
	20	13.54
C2-bentonite	3	14.42
	5	14.28
	10	14.03
	20	14.06
C6-bentonite	3	13.34
	5	13.24
	10	13.18
PTAB-bentonite	3	14.79
	5	14.64
	10	15.12
	20	14.98
Vinyl-bentonite	3	14.19
	5	14.81
	10	16.63
	20	14.69
MTPB-bentonite	3	15.41
	5	16.75
	10	16.89
	20	17.12

4.1.3   Characterization of organobentonite by FT-IR

The spectra of organoclays prepared with different concentrations of surfactants were recorded in the region of 4000-400 cm^{-1}. After modification with C-1, C-2 and C-6 the obtained organoclays showed the new bands at 2918, 2851 and 1487 cm^{-1} for C-1, 2924, 2851 and 1490 cm^{-1} for C-2 and 2959, 2862, 1488 and 1474 cm^{-1} for C-6, which resulting from the surfactants (see in Figure 4.8-4.10). The bands around 2900-2950 cm^{-1} and 2851-2862 cm^{-1} are assigned to asymmetric and symmetric stretching vibration of C-CH$_2$ of alkyl chain, respectively, and the band around 1487-1490 cm^{-1} is assigned to vibration of trimethylammonium quaternary group C-N(CH$_3$)$_3^+$ (Wong et al., 1997).
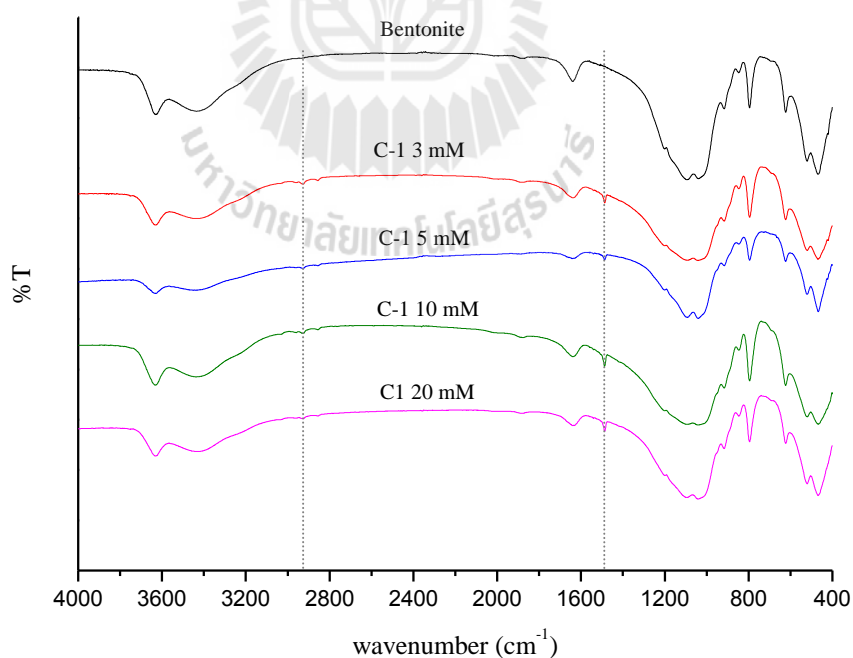
Figure 4.8 FTIR spectra of bentonite samples modified by different concentrations of tetramethylammonium hydroxide (C-1).
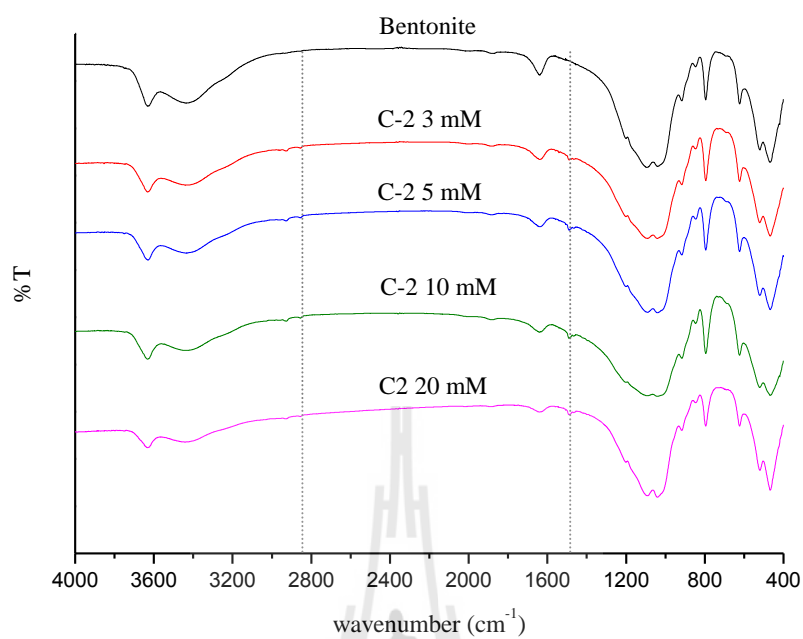
Figure 4.9 FTIR spectra of bentonite samples modified by different concentrations of

ethyltrimethylammonium iodide (C-2).
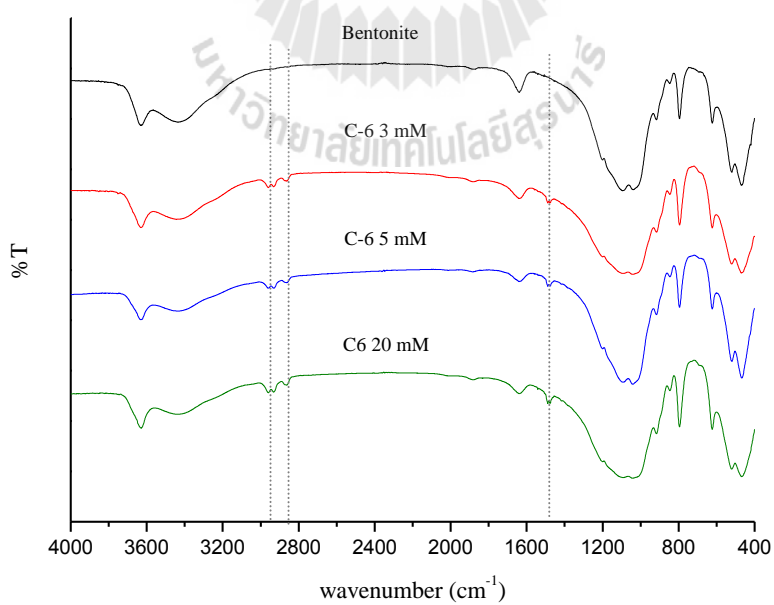
Figure 4.10 FTIR spectra of bentonite samples modified by different concentrations

of hexylmethylammonium bromide (C-6).

After modification of bentonite with PTAB, Vinyl and MPTB, the peaks in the range of 1400-1600 cm^{-1} were observed (see Figures 4.11-4.13). These peaks with low intensity are attributed to phenyl ring of the modifiers. It was confirmed that the modifiers were incorporated in the modified bentonite samples. The positions of these peaks are at 1498, 1462 and 1412 cm^{-1} for PTMA-bentonite, 1484, 1459 and 1396 cm^{-1} for Vinyl-bentonite and 1588, 1484 and 1440 cm^{-1} for MTPB-bentonite. The peaks in this range (1400-1600 cm^{-1}) exhibited the higher intensity of MPTB-bentonite more than the others due to MPTB consisting a greater number of phenyl rings.
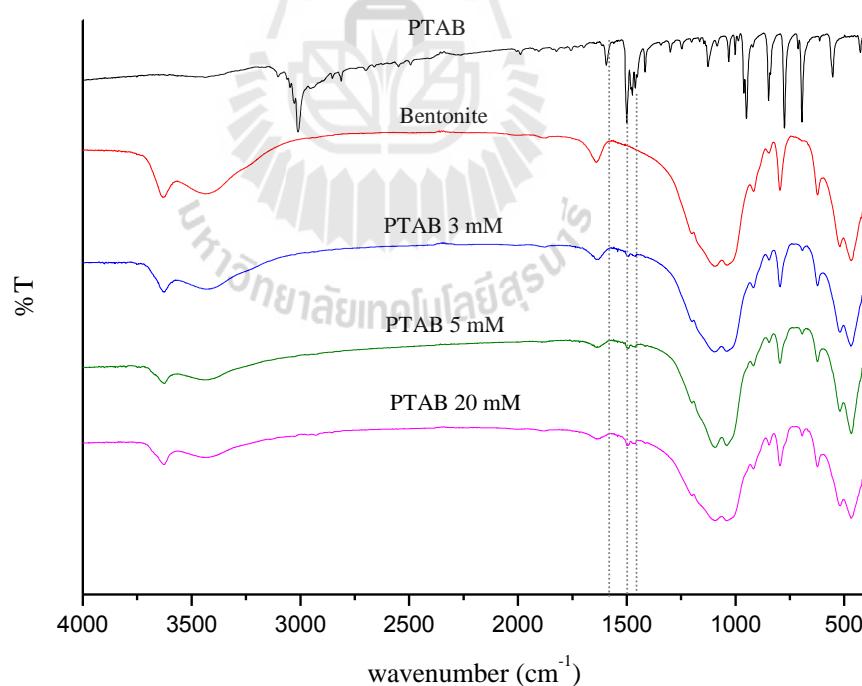
Figure 4.11 FTIR spectra of bentonite samples modified by different concentrations of phenyltrimethylammonium bromide (PTAB).
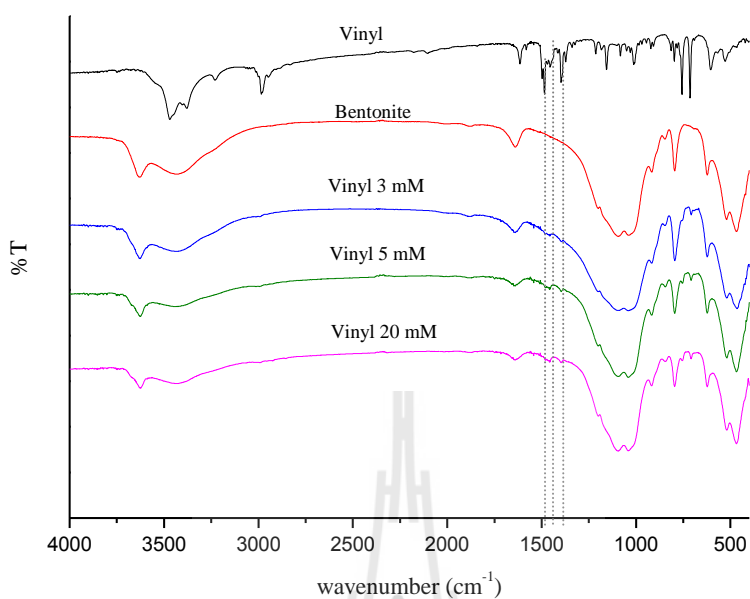
Figure 4.12 FTIR spectra of bentonite samples modified by different concentrations

of (vinylbenzyl)trimethylammonium chloride (Vinyl).
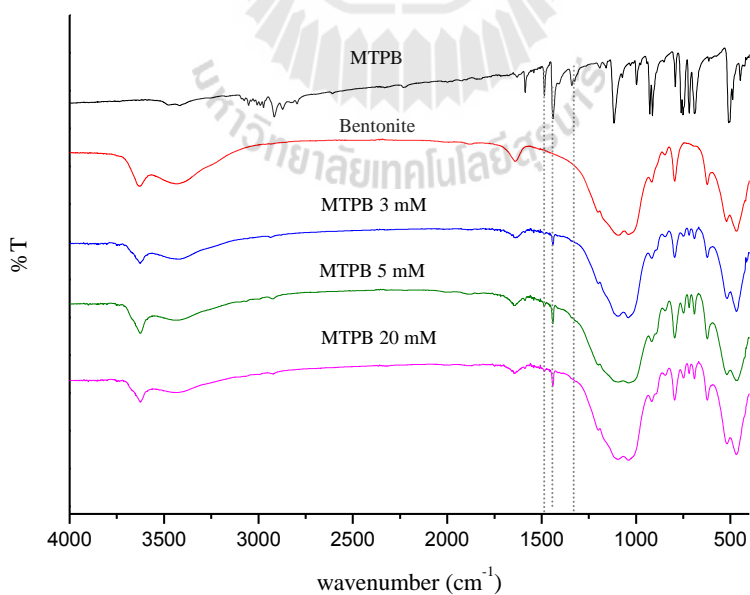
Figure 4.13 FTIR spectra of bentonite samples modified by different concentrations

of methyltriphenylphosphonium bromide (MTPB).

Table 4.2 Identification of IR bands of bentonite and modified bentonite samples.

Sample	IR absorption band (cm^{-1})	Band assignment
bentonite	3626	O-H
	1039	Si-O stretching
	622	Al-O, Si-O out of plan
	520	Al-O-Si bending
	469	Si-O-Si bending
C1-bentonite	2918	C-H asymmetric stretching
	2851	C-H symmetric stretching
	1487	C-H$_2$ scissoring
C2-bentonite	2924	C-H asymmetric stretching
	2851	C-H symmetric stretching
	1490	C-H$_2$ scissoring
C6-bentonite	2959	C-H asymmetric stretching
	2862	C-H symmetric stretching
	1488, 1474	C-H$_2$ scissoring
PTAB-bentonite	1498, 1462, 1412	Ring stretching
	1637	H–O–H bending vibration
Vinyl-bentonite	1484, 1459, 1396	Ring stretching
	1640	H–O–H bending vibration
MTPB-bentonite	1588, 1484, 1440	Ring stretching
	1647	H–O–H bending vibration

Source: Eren and Afsin, 2008; Wong et al., 1997.

4.1.4 Characterization of Al-pillared bentonite by XRD

The XRD patterns of bentonite and Al-pillared samples are displayed in Figure 4.14. A typical diffraction peak of bentonite is $2\theta = 5.92°$, corresponding to a basal spacing (d_{001}) of 15.08 Å. After intercalation with the Al_{13}- polyoxocation, the peak of PILC-1, PILC-2, PILC-3 PILC-4, PILC-5 and PILC-6 moves to lower angle (4.46°, 5.32°, 5.11°, 4.82°, 4.82° and 4.80°), corresponding to d_{001} of 17.83 Å, 16.60 Å, 17.28 Å, 18.30 Å, 18.31 Å and 18.37 Å, respectively. It is clear that an increase in basal spacing occurs in the presence of the Al_{13}-polyoxocation.
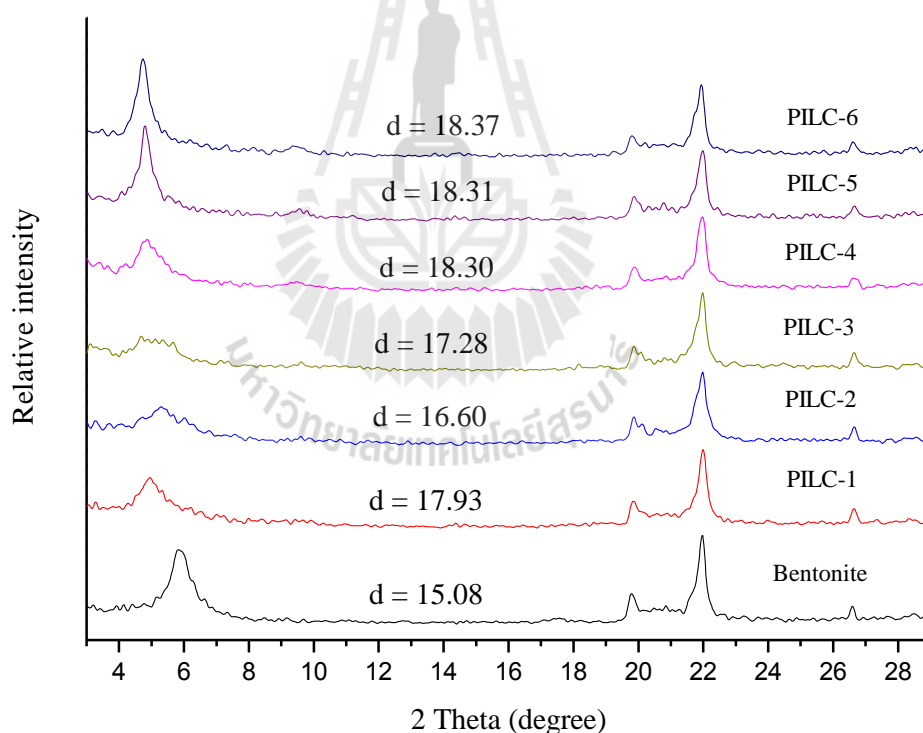
Figure 4.14 XRD patterns of PILCs prepared with different conditions.

4.1.5 Characterization of PCHs by FT-IR

FT-IR spectra of PCHs are shown in Figure 4.15. The peaks at 3632 cm^{-1} is a characteristic of bentonite corresponding to the fundamental stretching vibration of hydroxyl groups of Si-OH or Al-OH (Saini et al., 2011) and the peak at 1039 cm^{-1} is a characteristic of Si-O-Si stretching vibration of clay minerals. The peaks at around 3436 cm^{-1} and 1630-1637 cm^{-1} are stretching and bending vibration of water forming hydrogen bond, respectively. The spectra of PCHs were different from the starting bentonite indicated by the absence of peak at 3632 cm^{-1} and 1039 cm^{-1}. So it roughly infer that the structure of starting clay are changed after the modification. The sharp peak centered at about 1086-1091 cm^{-1} can be assigned to the stretching vibration of the SiO_4 units of the silicate layers (Nakatsuji et al., 2004)
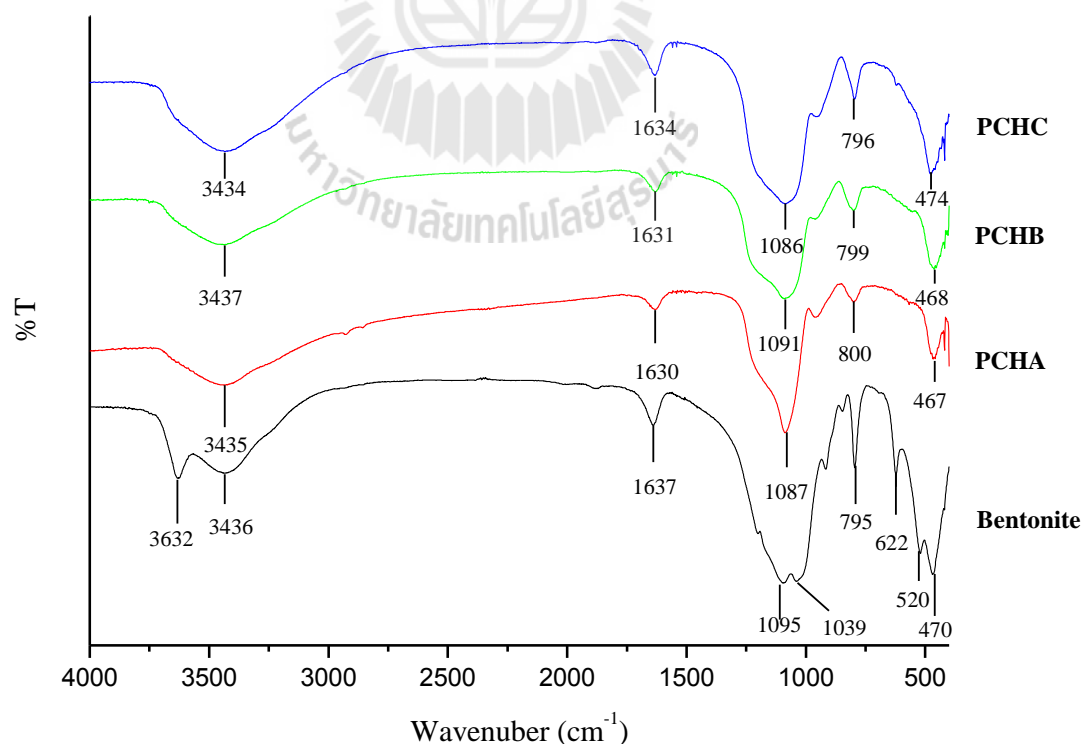
Figure 4.15 FT-IR patterns of bentonite, PCHA, PCHB and PCHC.

4.2 Surface area, pore volume and pore size

The information on particle analysis such as BET surface area, external surface area, micropore surface area, total pore volumes, micropore volumes and average pore diameters are summarized in Table 4.3.

Total BET surface area is the summation of external surface area and micropore surface area. From the obtained results, it was clearly seen that modified bentonite (C-2, PILCs and PCHs) had higher total BET surface area than unmodified bentonite. The isotherm of bentonite (Figure 4.16-4.19) shows a characteristic of non-porous solid due to its low surface area only 31.1 m^2/g. For PCHA, PCHB and PCHC the surface area is increased to ~897, 579 and 575 m^2/g, respectively. In the case of PILC-1, PILC-2, PILC-3, PILC-4, PILC-5 and PILC-6, the surface areas are increased to ~184, 138, 150, 178, 224 and 199 m^2/g, respectively. When compared the external surface area and the micropore surface area the major contribution to increase the surface area are mainly from an increase in micropore area. It is clear that the micropore surface area is depended upon the conditions of the preparation, indicating that the micropore structure was changed upon the modifications with poly-cationic at different conditions. This result indicated that large poly-cationic molecules can enter the interlayer of bentonite to form two dimensional micropore. Modifying bentonite with PTAB or TMPB showed no existence of micropore surface area which is similar to the result of bentonite. This may result from the blockage effect that is dependent on the structure of modifiers. When bentonite was modified with C-2, the micropore surface area occurred with an amount of 24.42 m^2/g and the external surface area (46.48 m^2/g) was increased compared to bentonite, PTAB-bentonite and TMPB-

bentonite. It may be due to the formation of two dimensional micropore in C2-
bentonite.

Table 4.3 Surface analysis of bentonite and modified bentionites.

sample	BET m^2/g	Pore volume (cm^3/g)	Micropore volume (cm^3/g)	Pore Diameter (nm)	Micropore surface (m^2/g)	External surface area (m^2/g)
Bentonite	31.1	0.18	0	2.35	0	31.1
20 mM C-2	70.9	0.22	0.01	1.24	24.4	46.5
20 mM PTAB	31.9	0.19	0	2.39	0	31.9
20 mM MTPB	28.7	0.17	0	2.35	0	28.7
PILC-1	184.8	0.30	0.07	6.47	132.9	51.9
PILC-2	138.7	0.32	0.04	9.18	89.0	49.7
PILC-3	150.1	0.22	0.05	5.73	101.5	48.6
PILC-4	178.4	0.30	0.06	6.73	125.7	52.7
PILC-5	224.7	0.37	0.09	6.62	164.0	60.7
PILC-6	199.7	0.33	0.07	6.63	140.6	59.1
PCHA	897.7	0.93	0.34	4.13	698.8	198.9
PCHB	579.2	0.79	0.12	5.46	252.4	326.8
PCHC	575.8	0.66	0.21	4.55	416.3	159.5
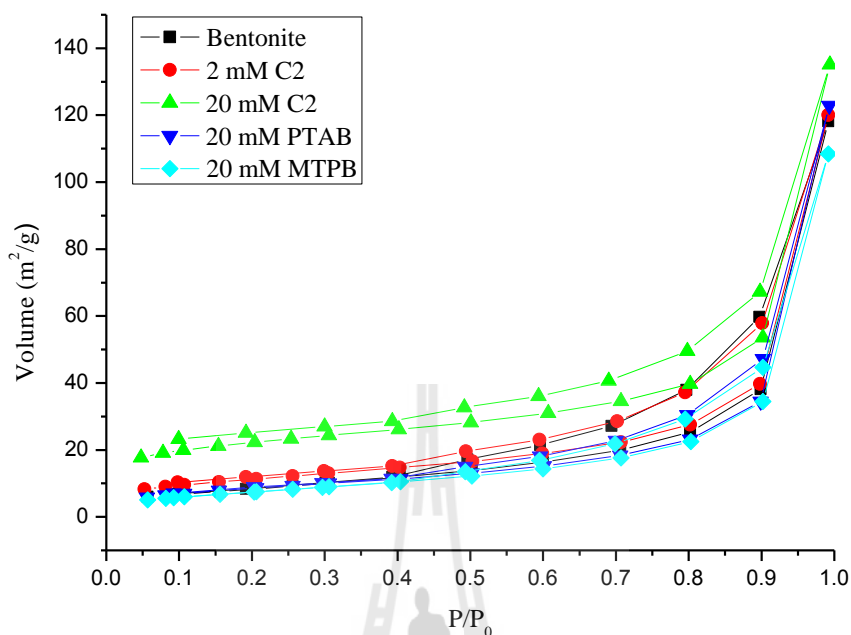
Figure 4.16 N_2 adsorption-desorption isotherms of of organoclay.
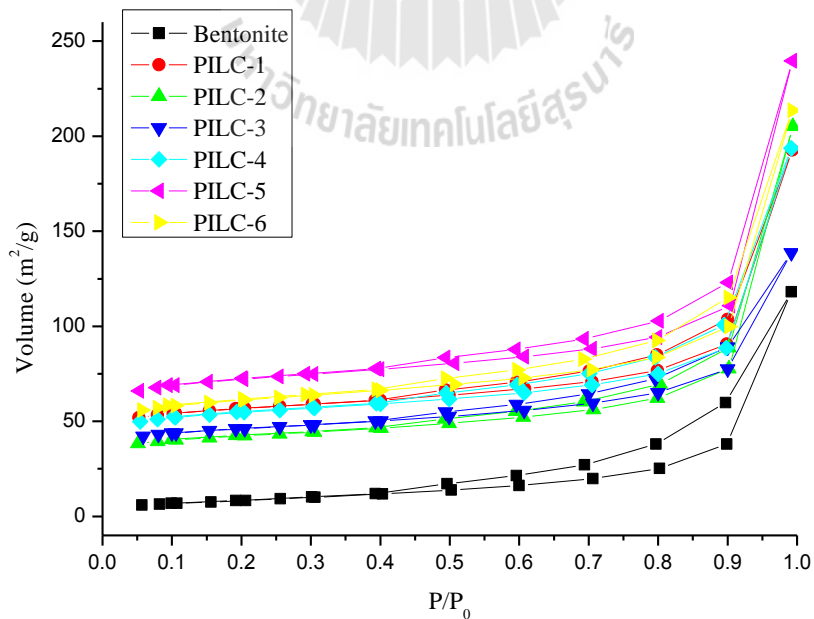
Figure 4.17 N_2 adsorption-desorption isotherms of of PILCs.
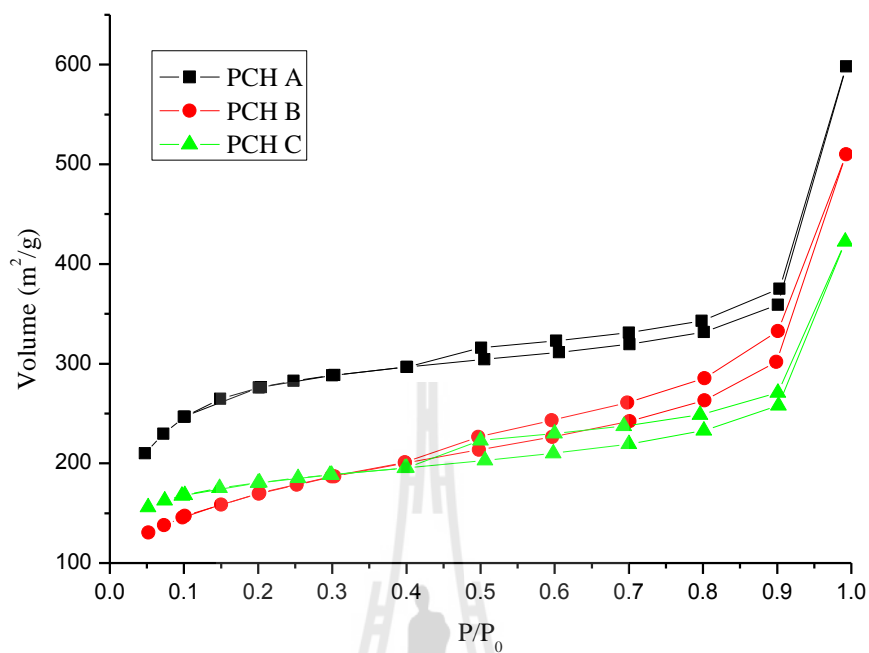
Figure 4.18 N_2 adsorption-desorption isotherms of of PCHs.
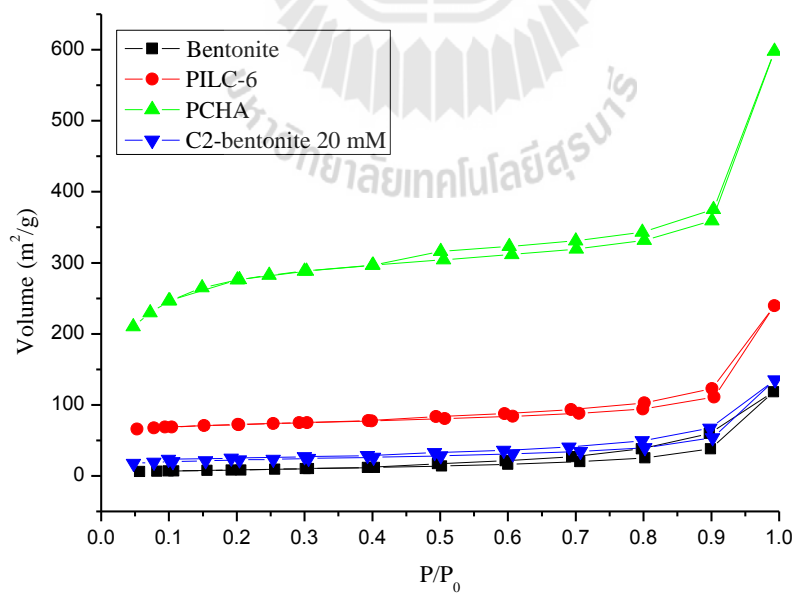
Figure 4.19 N_2 adsorption-desorption isotherms of bemtonite, PILC-6, PCHA and

C2-bentonite 20 mM.

4.3   Ethylene adsorption study

4.3.1   Ethylene adsorption on organoclay

In the study of ethylene adsorption with organoclays, HDTMA (C-16) was the first choice in the modification of clays. It was expected that organoclays (organokaolin, organohalloysite and organobentonite) could adsorb more ethylene due to their hydrophobicity. But these organoclays did not adsorb ethylene as expected. The ethylene capacities of organokaolin and organohalloysite were shown in Appendix. Then the modification with surfactants was continuously carried out by using surfactants with shorter tails (C-6, C-2, C-1) and also with one tail and three tails consisting of aromatic groups.

The ethylene adsorption isotherms of bentonite and cationic surfactant modified bentonite are shown in Figures 4.20-4.22. The adsorption capacity of bentonite was about 1 cm^3/g. When modified with C-6 in the concentrations of 3-10 mM, the ethylene adsorption capacity increased from ~ 1 to 2-5 cm^3/g depending on the concentration of C-6. (see Figure 4.22). After modification with C-1 and C-2 in the concentration range of 3 to 20 mM, adsorption of ethylene was higher than C6-bentonite (see Figures 4.22-4.21). At this time the adsorption capacity increased from ~ 1 to 13 cm^3/g. It could be explained that in organobentonite modified with shorter tail (shorter aliphatic chain) as C-1 and C-2, the spaces or two-dimensional micropores can be formed which was confirmed by the existence of micropore surface area (see Table 4.3) determined by BET surface analysis. Whereas the ethylene adsorption of bentonite occurred only on the external surface due to no existence of microrpore surface area (see Table 4.3) and ethylene adsorption capacity was found to be about 1 cm^3/g. It indicated that the micropore is almost reasonable for ethylene

adsorption. The van der Waals interaction of ethylene is very high in a space as micropore compared to a space as external surface. The lower ethylene adsorption capacity of C6-bentonite compared to C1-bentonite and C2-bentonite could be explained in term of blocking effect due to longer aliphatic chain of C-6. The more significant decrease in the ethylene adsorption capacity with an increase in the length of the tail may due to the greater blocking effect. In the case of the modification with HDTMA the ethylene adsorption was less than bentonite (about 0.3 cm^3/g). It may result from the greater blockage on the external and internal surface area of bentonite. In the case of ethylene adsored on the sheet of bentonite, it could be described by the possibility of the following interactions. A very weak hydrogen bond interaction of oxygen atom of clay and hydrogen atom of ethylene (CH…O) and a weak interaction of pi bond of ethylene with cations at the negative charge layer.
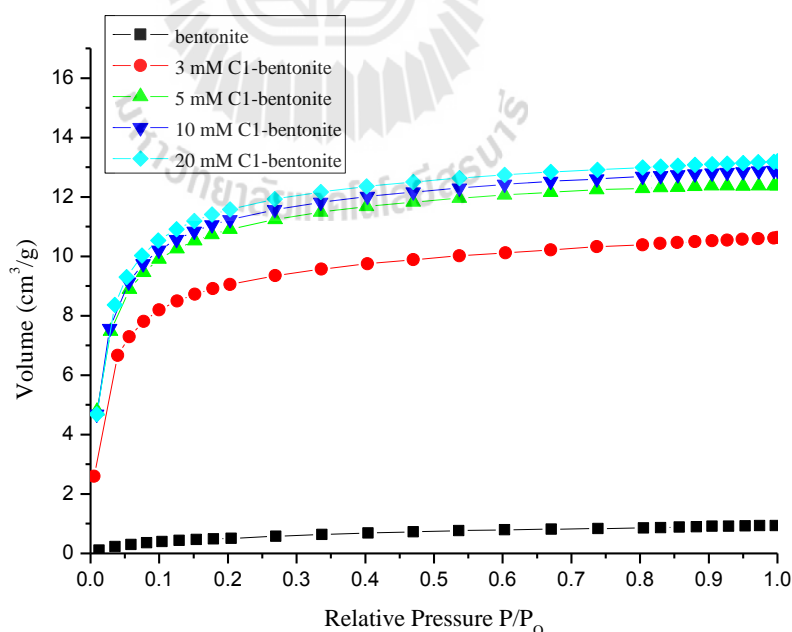
Figure 4.20 Ethylene adsorption isotherms of various concentrations of C-1 surfactant modified bentonite samples.
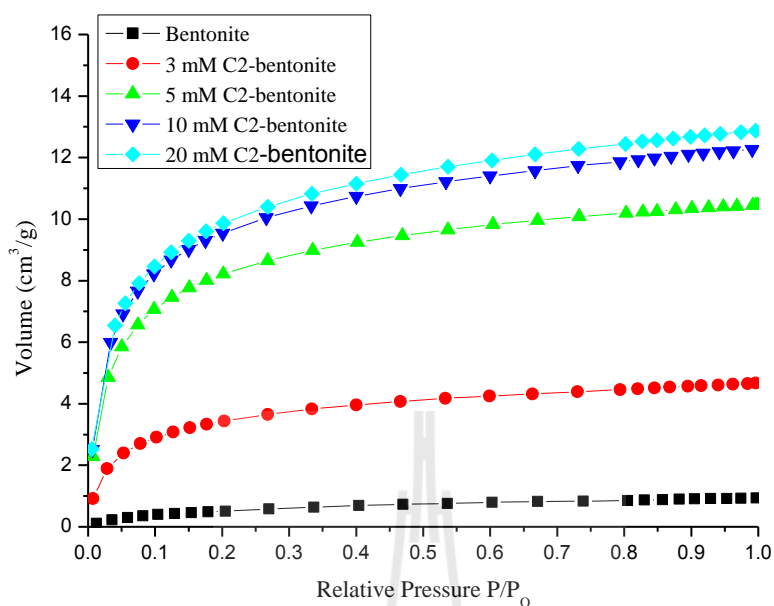
Figure 4.21 Ethylene adsorption isotherms of various concentrations of C-2 surfactant modified bentonite samples.
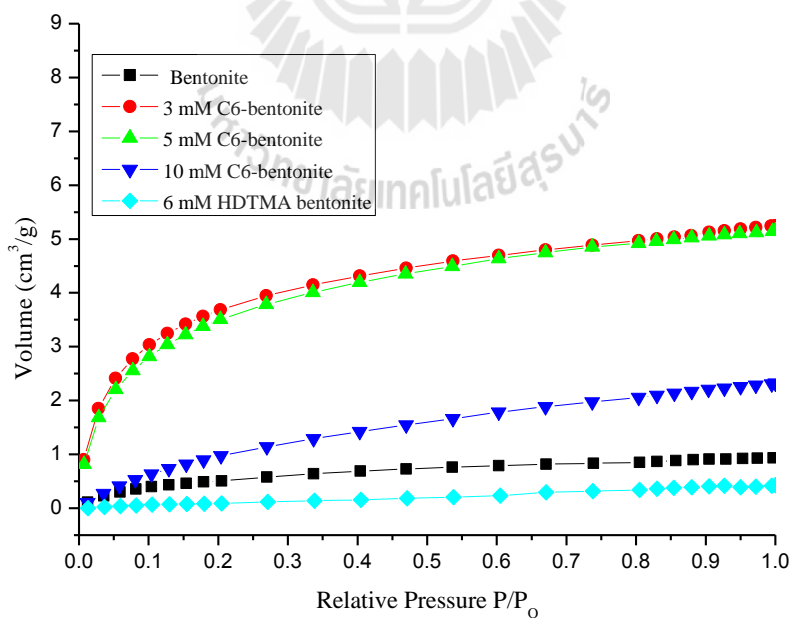
Figure 4.22 Ethylene adsorption isotherms of various concentrations of C-6 surfactant modified bentonite samples.

Again, when trying to modify betonite with PTAB (phenyltrimethylammonium bromide) in the concentration range of 3-20 mM (see Figure 4.23), the results showed that the ethylene adsorption capacity increased from 1 to 8 cm^3/g. The best adsorption was obtained by the adsorbent modified with 5 -20 mM of PTAB. From Table 4.3, it showed that the surface area of PTAB-bentonite was similar to bentonite, but its ethylene adsorption capacity was higher than bentonite. It was explained in terms of the additional interaction of PTAB-bentonite occurring in two fashions. One is the interaction between CH of ethylene and π-electron of phenyl ring in the tail part and another one is between CH of phenyl and π-electron of ethylene. CH…O and CH-π interactions are other interactions that can occur between ethylene and the surface of cationic surfactant modified bentonite. These interactions can be classified as weak hydrogen bonds. Therefore, PTAB modified bentonite can adsorb ethylene better than unmodified bentonite.

When trying to modify bentonite with methyltriphenylphosphonium bromide (TMPB), we expected that the higher capacity of ethylene adsorption should be obtained with these TMPB-bentonites due to TMPB consisting three phenyl rings. TMPB-bentonite should have more adsorption sites due to the greater number of phenyl rings. The interactions between ethylene and TMPB-bentonite were considered to be the same as PTAB. However, the results showed the opposite to our expectations (see Figure 4.24). The highest amount of ethylene adsorbed by TMPB-bentonite with 3 mM was only 3 cm^3/g. The lower amount of ethylene could be adsorbed with an increase in the concentration of TMPB. It may be the result of the blockage effect that is more pronounce than the increases of interaction sites. Figure 4.25 shows the ethylene adsorption by bentonite modified with

(vinylbenzyl)trimethylammonium chloride in the concentration range of 3-20 mM. The result was similar to the adsorption of TMPB-bentonite. Figure 4.26 shows the ethylene adsorption isotherms of the different organobentonites. At this time the best organobentonites were obtained by bentonite modified with the short aliphatic chain of C-1 or C-2 of quaternary ammonium with the adsorption capacity of about 13 cm^3/g.
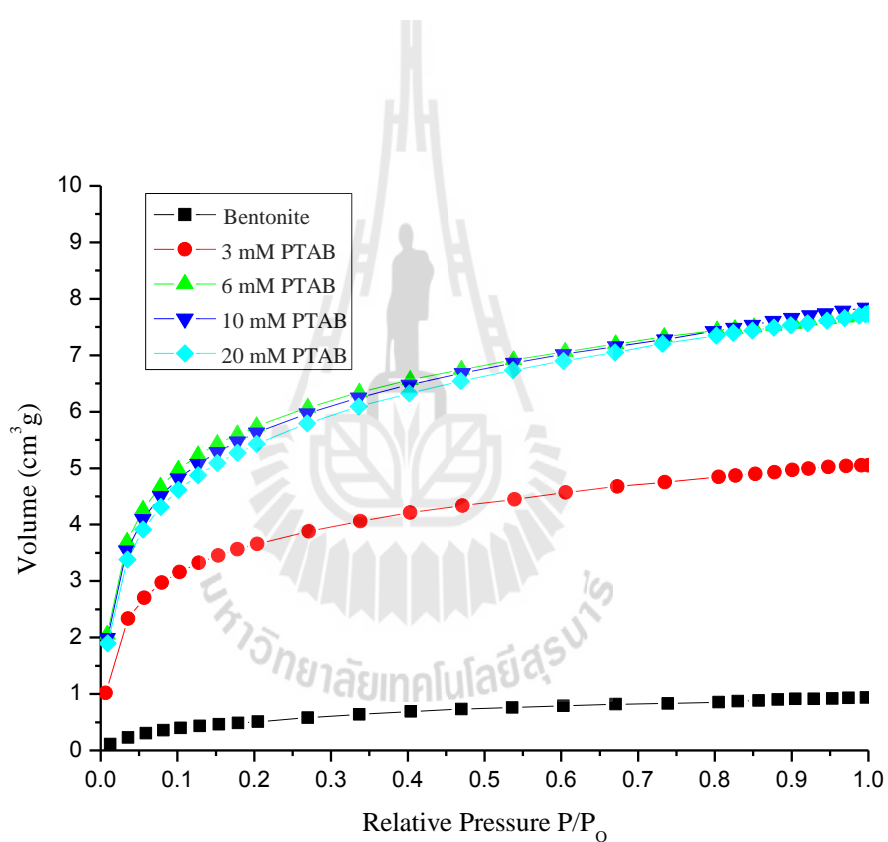
Figure 4.23 Ethylene adsorption isotherms of various concentrations of PTAB surfactant modified bentonite samples.
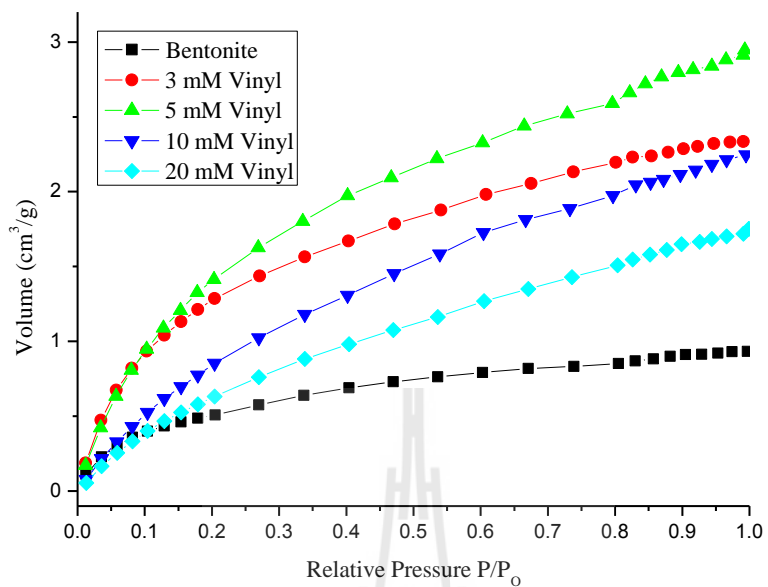
Figure 4.24 Ethylene adsorption isotherms of various concentrations of vinyl surfactant modified bentonite samples.
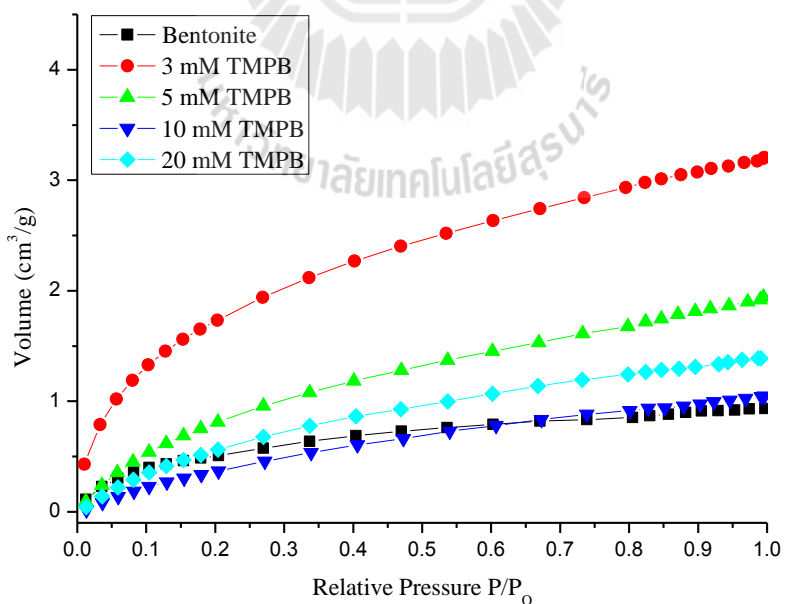
Figure 4.25 Ethylene adsorption isotherms of various concentrations of TMPB surfactant modified bentonite samples.
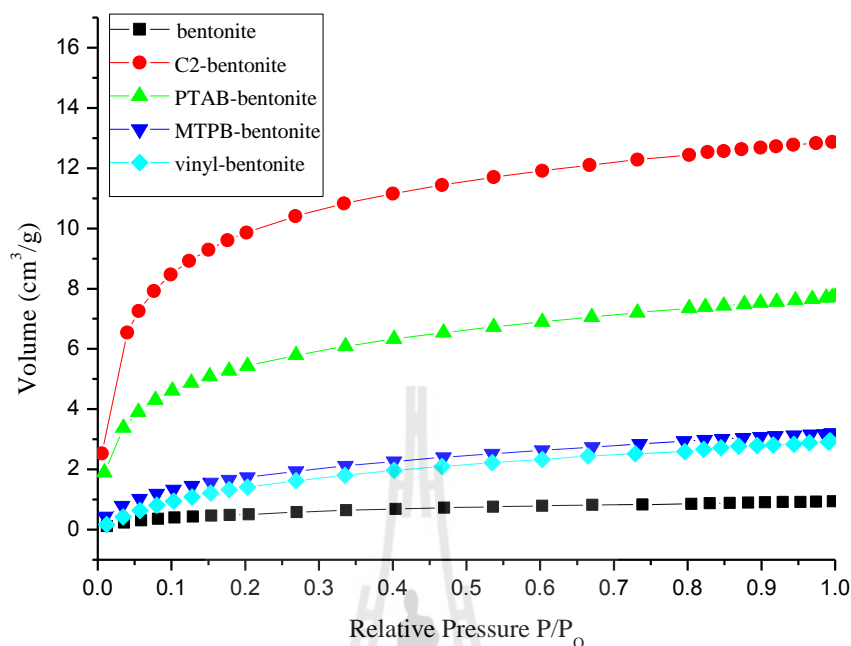
Figure 4.26 Ethylene adsorption isotherms of different surfactants modified bentonite samples.

4.3.2 Ethylene adsorption on PILCs

The ethylene adsorption isotherms of all PILCs prepared under different conditions are shown in Figure 4.27. The results showed that the ethylene adsorption capacity increased from about 1 cm^3/g for bentonite to 9-13 cm^3/g for all PILCs. The isotherms shows that the adsorption capacity of PILC-5 and PILC-6 were higher than those of PILC-1, PILC-2, PILC-3 and PILC-4. The adsorbed amount tends to increase with the surface area of the PILCs determined by nitrogen adsorption (see Table 4.4). The higher the surface area is, the more ethylene is adsorbed. The ethylene adsorption capacities of PILC-5 and PILC-6 are comparable to those of organobentonites modified with C-1 and C-2.

Table 4.4 Surface areas of PILCs and their ethylene adsorption capacities.

Sample	BET (m^2/g)	Ethylene adsorption (cm^3/g)
PILC-1	184.8	11.56
PILC-2	138.7	9.85
PILC-3	150.1	9.16
PILC-4	178.4	11.33
PILC-5	224.7	12.89
PILC-6	199.7	12.79
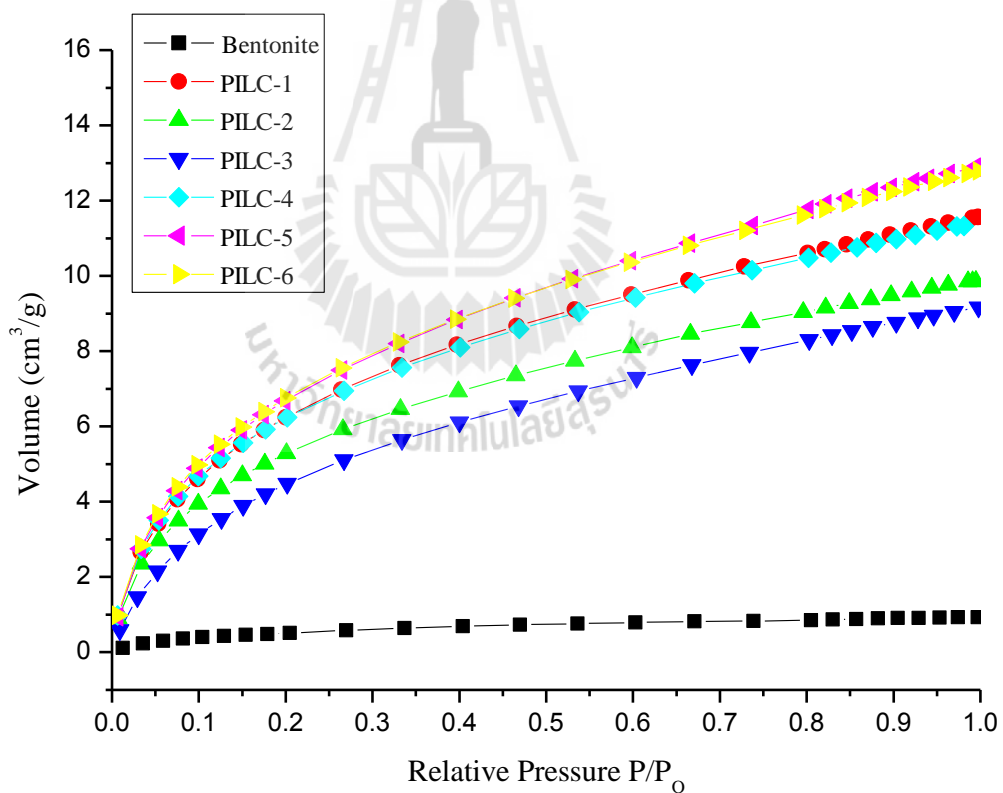
Figure 4.27 Ethylene adsorption isotherms of PILCs.

4.3.3 Ethylene adsorption on PCHs

The ethylene adsorption isotherms of all PCHs are shown in Figure 4.28. It was found that the prepared PCHA can adsorb ethylene better the others. In this study the sample of PCHA was found to be the best adsorbent for ethylene adsorption. Its capacity was 32 cm^3/g. The adsorption capacities increased from 1 cm^3/g (bentonite) to 25-32 cm^3/g (PCHs). Table 4.5 shows that the ethylene adsorption capacity depends on the surface area. The larger surface area of PCHA results in the higher ethylene adsorption capability.

Table 4.5 Surface areas of PCHs and their ethylene adsorption capacities.

Sample	BET (m^2/g)	Ethylene adsorption (cm^3/g)
PCHA	897.7	32.19
PCHB	579.2	25.03
PCHC	575.8	26.36
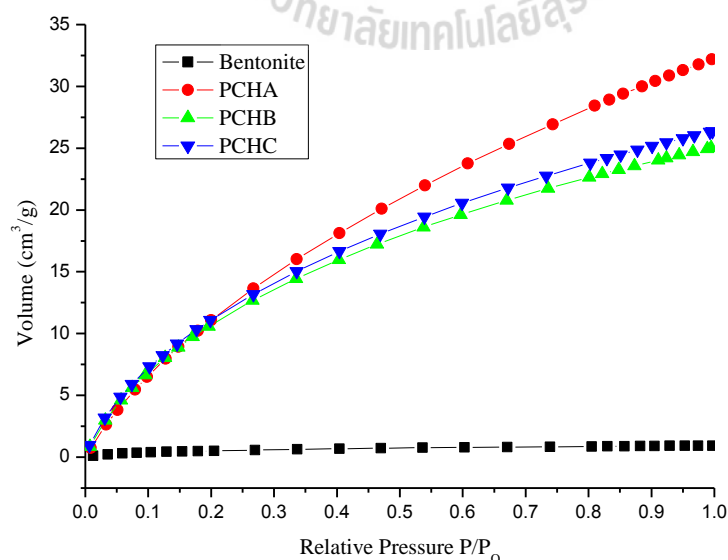
Figure 4.28 Ethylene adsorption isotherms of PCHs.
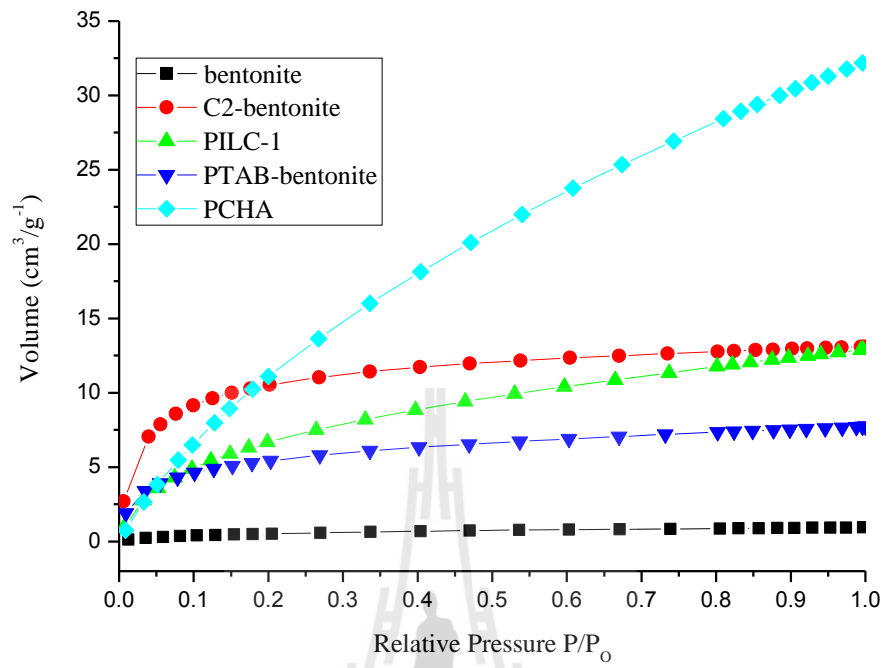
Figure 4.29 Ethylene adsorption isotherms of bentonite and modified bentonites with

different methods.

CHAPTER V

CONCLUSION

This work focused on modifications of bentonite to produce materials which can adsorb ethylene. In this work bentonite was modified to be namely organoclay, pillared clay (PILC) and porous clay heterostructure material (PCH).

Organoclay was prepared by modifying bentonite with cationic surfactants (C-1, C-2, C-6 HDTMA, PTAB, Vinly and MTPB). The characterizations of the modified samples were determined by XRD, FT-IR and BET surface area analysis technique. The XRD indicated that the bentonite modified with C-1, C-2, C-6, PTAB and Vinyl, the basal spacing of d_{001} were decreased. The decrease in the basal spacing of d_{001} may be caused by an attractive intermolecular forces between the neighboring sheet, due to the structure of the modifiers, sufficiently to keep the sheets close together. In the case of bentonite modified with MTPB, the d_{001} was increased with an increase in MTPB concentrations. It was expanded from 15.08 to 17.12 Å indicating that MTPB was incorporated into the interlayer of bentonite. FT-IR showed the bands of the modifiers indicating that all modifiers can incorporate to bentonite. The bands in the range of 1400–1600 cm^{-1} are due to C-H bending and C=C stretching, indicating existence of alkyl chain and aromatic ring in organobentonite. The intercalation of PILCs with the Al_{13}- polyoxocation showed the basal spacing of d_{001} was increased from 15.08 (bentonite) to 18.37 Å. It was indicated that an increase in basal spacing occurs in the presence of the Al_{13}-polyoxocation. The IR-spectra of PCHs exhibited the absence of the characteristic peaks of bentonite (3632 cm^{-1} and 1039 cm^{-1})

indicating that bentonite was totally changed into PCHs with very high surface areas of 575.8-897.7 m^2/g. While the IR band of PILCs still showed the characteristic peaks of bentonite. The surface area of PILCs was 138.7-224.7 m^2/g whereas the surface area of betonite was 31.1 m^2/g.

In the ethylene adsorption, it was found that the capable of adsorbing ethylene gas with C1-bentonite, C2-bentonite and PILC was in the same level about 13 cm^3g^{-1}. While the maximum of ethylene adsorption capacity of PCH was about 32 cm^3g^{-1}. The ethylene adsorption capacity of the modified bentonites could be explained in terms of the surface area of the materials especially micropore surface area and blockage effect. The interactions of ethylene and modified bentonites could be described as follows. A very weak hydrogen bond beween oxygen atom of clay and hydrogen atom of ethylene (CH…O) and a weak interaction of π bond of ethylene with cations of clay.
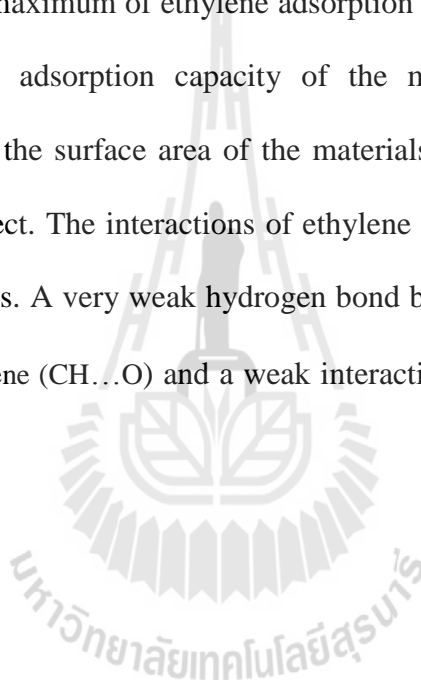
REFERENCES

REFERENCES

Abe, K., and Watada, A. E. (1991). Ethylene adsorbent to maintain quality of lightly processed fruits and vegetables. **Journal of Food Science**. 56: 1589-1592.

Al-Baghli, N. A., and Loughlin, K. F. (2006). Binary and ternary adsorption of methane, ethane, and ethylene on titanosilicate ETS-10 zeolite. **Journal of Chemical and Engineering Data**. 51: 248-254.

Alkaram, F. U., Mukhlis, A. A., and Al-Dujaili, H. A. (2009). The removal of phenol from aqueous solutions by adsorption using surfactant-modified bentonite and kaolinite. **Journal of Hazardous Materials**. 169: 324-332.

Anson, A., Wang, Y., Lin, C. C. H., Kuznicki, T. M., and Kuznicki, S. M. (2008). Adsorption of ethane and ethylene on modified ETS-10. **Chemical Engineering Science**. 63: 4171-4175.

Arellano-Cardenas, F., Gallardo-Velazquez1, T., and Osorio-Revilla, G. (2007). Preparation of a porous clay heterostructure and study of its adsorption capacity of phenol and chlorinated phenols from aqueous solutions. **Water Environment Research**. 80: 60-70.

Bergaya, F., Theng, B. K. G., and Lagaly, G. (2006). **Handbook of Clay Science**. Amsterdam: Elsevier Science. pp. 327-330.

Berlier, K., Olivier, M. G., and Jadot, R. (1995). Adsorption of methane, ethane, and ethylene on zeolite. **Journal of Chemical Engineering**. 40: 1206-1208.

Bonczek, J. L., Harris, W. G., and Nkedi, K. P. (2002). Monolayer to bilayer transitional arrangements of hexadecyltrimethylammonium cations on Na-montmorillonite. **Clays and Clay Minerals**. 50: 11-17.

Bouras, O., Chami, T., Houari, M., Khalaf, H., Bollinger, J. C., and Baudu, M. (2002). Removal of sulfacid brilliant pink from an aqueous stream by adsorption onto surfactant modified Ti-pillared montmorillonite. **Environmental Technology**. 23: 405-411.

Cheng, L. S., and Yang, R. T. (1995). Monolayer cuprous chloride dispersed on pillared clays for olefin-paraffin separations by π-complexation. **Adsorption**. 1: 61-75.

Choi, B., Choi, D., Lee, Y., and Lee, B. (2003). Adsorption equilibria of methane, ethane, ethylene, nitrogen, and hydrogen onto activated carbon. **Journal of Chemical Engineering**. 48: 603-607.

Chow, B., and McCourt, P. (2006). Plant hormone receptors: Perception is everything. **Genes and Development**. 20(15): 1998-2008.

Clauer, N., and Chaudhuri, S. (1995). Clay in crustal environments. **Fundamentals of Clay Mineralogy**. 514: 12-13.

Cool, P., and Vansant, E. F. (1998). Pillared clays: Preparation, characterization and applications. **Molecular Sieves**. 1: 265-288.

Danis, T. G., Albanis, T. A., Petrakis, D. E., and Pomonis, P. J. (1998). Removal of chlorinated phenols from aqueous solutions by adsorption on alumina pillared clays and mesomorphous alumina aluminum phosphate. **Water Research**. 32: 295-302.

Department of Chemistry, Northern Kentucky University. (2012). **Introduction to X-ray Diffraction**. [Online]. Available: http://www.asdlib.org/onlineArticles/ ecourseware/Bullen XRD/XRDModule Theory Instrument%20Design 3.htm.

Do, D. D. (1998). **Adsorption Analysis: Equilibria and Kinetic.** London UK: Imperial College Press. pp. 80-112.

Eldridge, R. B. (1993). Olefin/paraffin separation technology: A review. **Industrial and Engineering Chemistry Research**. 32: 2208-2212.

El-Nahhal, Y., Nir, S., Polubesova, T., Margulis, L., and Rubin, B. (1998). Leaching, phytotoxicity and weed control of new formulations of alachlor. **Journal of Agricultural and Food Chemistry**. 46: 3305-3313.

Erdogan, B., Sakızci, M., and Yorukogullari, E. (2008). Characterization and ethylene adsorption of natural and modified clinoptilolites. **Applied Surface Science**. 254: 2450-2457.

Eren, E., and Afsin, B. (2008). An investigation of Cu(II) adsorption by raw and acid-activated bentonite: A combined potentiometric, thermodynamic, XRD, IR, DTA study. **Journal of Hazardous Materials**. 151: 682-691.

Gitipour, S., Bowers, M. T., and Bodocsi, A. (1997). The use of modified bentonite for removal of aromatic organics from contaminated soil. **Journal of Colloid and Interface Science**. 196: 191-198.

Grim, R. E. (1953). **Clay Mineralogy**. New York: McGraw-Hill. pp. 50-79.

Izumi, Y., Urabe K., and Onaka M. (1992). **Zeolite, Clay and Heteropoly Acid in Organic Reaction**. Weinheim: VCH Verlagsgesellschaft. pp. 49-52.

Johnston, C. T., Sposito, G., and Erickson, C. (1992) Vibrational probe studies of water interactions with montmorillonite. **Clays and Clay Minerals**. 40: 722-730.

Kukkadapu, R. K., and Boyd, S. A. (1995). Tetramethylphosphonium- and tetramethylammonium-smectites as adsorbents of aromatic and chlorinated hydrocarbons: Effect of water on adsorption efficiency. **Clays and Clay Minerals**. 43: 318-323.

Lagaly, G. (1982). Layer charge heterogeneity in vermiculites: Clays. **Clays and Clay Minerals**. 30: 215-222.

Lawrence, M. A. M., Kukkadapu, R. K., and Boyd, S. A. (1998). Adsorption of phenol and chlorinated phenols from aqueous solution by tetramethylammonium- and tetramethylphosphonium-exchanged montmorillonite. **Applied Clay Science**. 13: 13-20.

Lewis, D. W., and McConchie, D. (1994). **Analytical Sedimentology**. London; New York: Champman & Hall. pp. 144-145.

Ma, J., and Zhu, L. (2006). Simultaneous sorption of phosphate and phenanthrene to inorgano-organo-bentonite from water. **Journal of Hazardous Materials**. 136: 982-988.

Madejov′a, J. (2003). FTIR techniques in clay mineral studies. **Vibrational Spectroscopy**. 31: 1-10.

Maes, N., and Vansant,. E. F. (1995). Study of Fe_2O_3-pillared clay synthesized using the trinuclear Fe(III)-acetato complex as pillaring precursor. **Microporous Materials**. 4: 43-51.

Majdan, M., Bujacka, M., and Sabah, E. (2009). Unexpected difference in phenol sorption on PTMA- and BTMA-bentonite. **Journal of Environmental Management**. 91: 195-205.

Maksimov, R. D., Gaidukovs, S., and Kalnins, M. (2006). A nanocomposite based on a styrene-acrylate copolymer and native montmorillonite clay 1. Preparation, testing, and properties. **Mechanics of Composite Materials**. 42: 45-54.

Marguls, L., Rozen, H., and Nir, S. (1988). Model for competitive adsorption of organic cations on clays. **Clays and Clay Minerals**. 36: 270-276.

Nakatsuji, M., Ishii, R., and Wang, Z., (2004). Preparation of porous clay minerals with organic–inorganic hybrid pillars using solvent-extraction route. **Journal of Colloid and Interface Science**. 272: 158-166.

Olson, C. G., Thompson, M. L., and Wilson, M. A. (2000). Phyllosilicates. In: **Handbook of Soil Science**. Sumner, M. E. (ed.). Boca Raton, Florida: CRC Press. pp. F77-F119.

Patdhanagul, N., Srithanratana, T., Rangsriwatananon, K., and Hengrasmee, S. (2010). Ethylene adsorption on cationic surfactant modified zeolite NaY. **Microporous and Mesoporous Materials**. 131: 97-102.

Pinto, M. L., and Rocha, J. (2008). Porous materials prepared from clays for the upgrade of landfill gas. **Journal of Physical Chemistry**. 112: 14394-14402.

Pires, J., Araujo, A. C., Carvalho, A. P., Pinto, M. L., Gonzalez-Calbet, J. M., and Ramırez-Castellanos, J. R. (2004). Porous materials from clays by the gallery template approach: Synthesis, characterization and adsorption properties. **Microporous and Mesoporous Materials**. 73: 175-180.

Pires, J., Saini, V., and Pinto, M. (2008). Studies on selective adsorption of biogas components on pillared clays: Approach for biogas improvement. **Environmental Science and Technology**. 42: 8727-8732.

Quantachrome Instruments. (2010). **Autosorb-1 Series Surface Area and Pore Size Analyzers**. [Online]. Available: http://www.quantachrome.com/gassorption/ retired/autosorb1_series_detail.html.

Richards, S., and Bouazza, A. (2007). Phenol adsorption in organo-modified basaltic clay and bentonite. **Applied Clay Science**. 37: 133-142.

Russell, J. D., and Fraser, A. R. (1994). IR. In: **Clay Mineralogy: Spectroscopic and Chemical Determinative Methods**. Wilson, M. J. (ed.). London: Chapman & Hall. pp. 11-38.

Saini, V. K., Pinto, M., and Pires, J. (2011). High pressure adsorption studies of ethane and ethylene on clay-based adsorbent materials. **Separation Science and Technology**. 46: 137-146.

Shmuel, Y., and Harold, C. (2002). **Organo-clay Complexes and Interaction**. New York: Marcel Dekker. pp. 1-49.

Spark, D. L. (1995). **Environmental soil chemistry**. San Diego: Academic Press.

Srinivasan, K. R., and Fogler, S. H. (1990). Use of inorgano-organo clays in the removal of priority pollutants from industrial wastewaters: Adsorption of benzo(α)-pyrene and chlorophenols from aqueous solutions. **Clays and Clay Minerals**. 38: 287-293.

Upson, R. T., and Burns, S. E. (2006). Sorption of nitroaromatic compounds to synthesized organoclays. **Journal of Colloid and Interface Science**. 297: 70-76.

Velde, B. (1992). **Introduction to Clay Minerals: Chemistry, Origins, Uses, and Environmental Significance**. London; New York: Champman & Hall. pp. 20-23.

Wang, C. C., Juang, L. C., Lee, C. K., Hsu, T. C., Lee, J. F., and Chao, H. P. (2004). Effects of exchanged surfactant cations on the pore structure and adsorption characteristics of montmorillonite. **Journal of Colloid and Interface Science**. 280: 27-35.

Wibulswas, R., White, D. A., and Rautiu, R. (1999). Adsorption of phenolic compounds from water by surfactant-modified pillared clays. **Institution of Chemical Engineerings Trans**. 77(B): 88-92.

Wilson, M. J. (ed.). Infrared methods In: **A Handbook of Determinative Methods in Clay Mineralogy**. Blackie, London. UK. pp. 133-173.

Wong, T. C., Wong, N. B., and Tanner, P. A. (1997). A fourier transform IR study of the phase transitions and molecular order in the hexadecyltrimethylammonium sulfate/ water system. **Journal of Colloid and Interface Science**. 186: 325-331.

Wu, P. X., Liao, Z. W., Zhang, H. F., and Guo, J. G. (2001). Adsorption of phenol on inorganic-organic pillared montmorillonite in polluted water. **Environment International**. 26: 401-407.

Yan, L., Shan, X., Wen, B., and Owens, G. (2008). Adsortion of cadmium onto Al_{13}-pillared acid-activated montmorillonite. **Journal of Hazardous Materials**. 156: 499-508.

Yang, R. T., and Kikkinides, E. S. (1995). New sorbents for olefin/paraffin separations by adsorption via π-complexation. **Institution of Chemical Engineerings Trans**. 41: 509-517.

Yapar, S., Özbudak, V., Dias, A., and Lopes, A. (2005). Effect of adsorbent concentration to the adsorption of phenol on hexadecyl trimethyl ammonium-bentonite. **Journal of Hazardous Materials**. 121: 135-139.

Zielke, R. C., and Pinnavaia, T. J. (1988). Modified clays for the adsorption of environmental toxicants: Binding of chlorophenols to pillared, delaminated, and hydroxyl interlayered smectites. **Clays and Clay Minerals**. 36: 403-408.
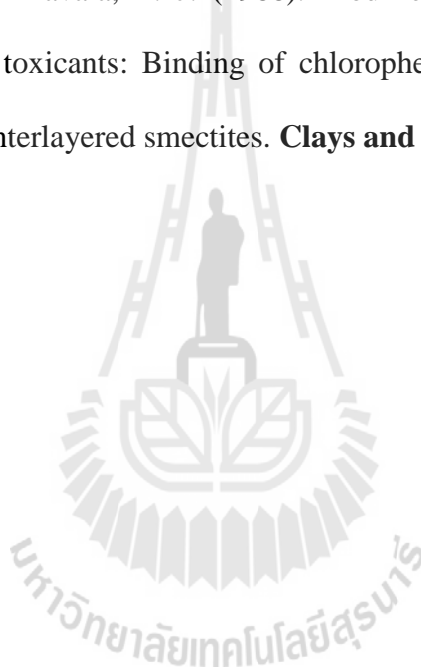
APPENDIX

APPENDIX

Table 1 Ethylene adsorption capacity of bentonite.

Clay	Modify	Adsorption (cm^3/g)
	-	0.9949
	2 mM PTAB	5.4200
	3 mM PTAB	7.2600
	4 mM PTAB	8.3934
Bentonite	5 mM PTAB	7.7124
	6 mM PTAB	8.9431
	12 mM PTAB	0.3670
	6 mM HDTMA	0.4291
	1 M KCl	0.9865

Table 2 Ethylene adsorption capacity of halloysite.

Clay	Modify	Adsorption (cm^3/g)
	-	1.5455
	6 mM PTAB	1.2421
Halloysite	12 mM PTAB	1.4891
	6 mM HDTMA	0.3551

Table 3 Ethylene adsorption capacity of kaolinite.

Clay	Modify	Adsorption (cm^3/g)
	-	0.6173
	6 mM PTAB	0.6770
Kaolinite	12 mM PTAB	0.7599
	6 mM HDTMA	0.5023

Table 4 Ethylene adsorption capacity of bentonite modified with metal.

Clay	Modify	Adsorption (cm^3/g)
	0.1 M $NiCl_2$	0.2322
	0.1 M $CoCl_2$	0.7406
	0.1 M $CuCl_2$	-
	0.1 M $ZnCl_2$	0.3398
Bentonite	0.1 M $NiCl_2$ + 4 mM PTAB	4.6611
	0.1 M $CoCl_2$ + 4 mM PTAB	9.9870
	0.1 M $CuCl_2$ + 4 mM PTAB	10.2738
	0.1 M $ZnCl_2$ + 4 mM PTAB	8.4733

Table 5 Ethylene adsorption capacity of halloysite modified with metal.

Clay	Modify	Adsorption (cm^3/g)
	0.1 M NiCl$_2$	-
	0.1 M CoCl$_2$	1.0603
	0.1 M CuCl$_2$	0.6473
	0.1 M ZnCl$_2$	0.9177
Halloysite	0.1 M NiCl$_2$ + 4 mM PTAB	1.1832
	0.1 M CoCl$_2$ + 4 mM PTAB	0.4726
	0.1 M CuCl$_2$ + 4 mM PTAB	1.4291
	0.1 M ZnCl$_2$ + 4 mM PTAB	0.9887

Table 6 Ethylene adsorption capacity of bentonite modified with Phenol.

Clay	Modify	Adsorption (cm^3/g)
	4 mM Phenol	0.8625
	8 mM Phenol	5.1426
Bentonite	20 mM Phenol	0.5094
	0.2 M Phenol	0

CURRICULUM VITAE

NAME: Mr. Saran Youngjan **DATE OF BIRTH:** September 19, 1985.

PLACE OF BIRTH: Sisaket, Thailand.

EDUCATIONAL BACKGROUND:

2008   Bachelor of Science (Chemistry)

Ubon Ratchathani Rajabhat University, Ubon Ratchathani, Thailand.

WORK EXPERIENCE:

2011-2012   Teaching Assistance, School of Chemistry, Institute of Science, Suranaree University of Technology, Nakhon Ratchasima.

PRESENTATION:

2013   Poster presentation "Ethylene adsorption on modified bentonite" Pure and Applied Chemistry International Conference (PACCON 2013), January 23-25, 2013, Burapha University, Bangsaen Chonburi, Thailand

.